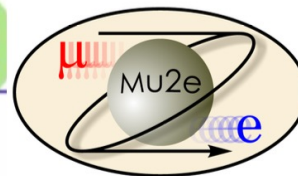


A data-driven method to estimate the antiproton background in the Mu2e experiment

Multi-track event reconstruction & other service tasks

Namitha Chithirasreemadam
namitha@pi.infn.it

Dipartimento di Fisica 'Enrico Fermi'
Università di Pisa,
INFN, Pisa



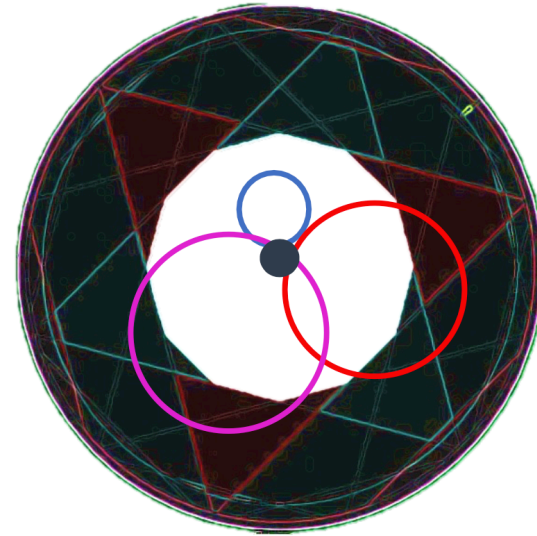
Background processes to $\mu^- \rightarrow e^-$ search

Decay in Orbit

- In free μ^- decay, e^- kinematic endpoint is $m_\mu/2$ and follows Michel spectrum.

$$R = \frac{p \perp}{qB} = 35 \text{ cm}$$

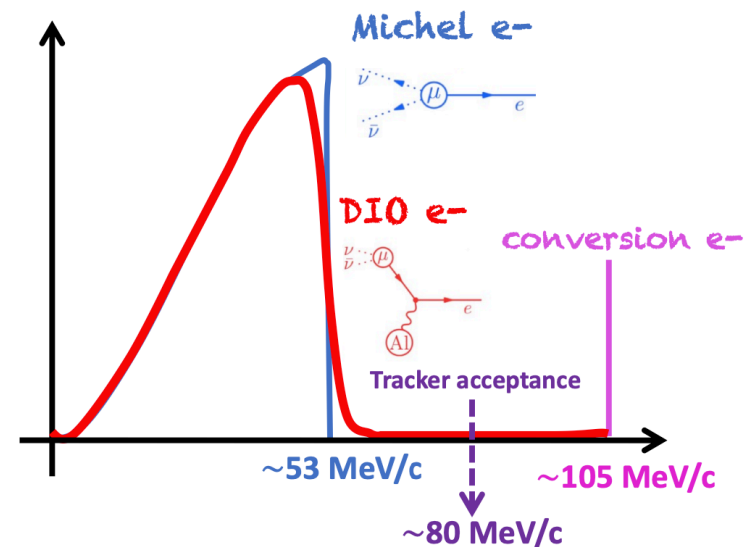
- In the field of a nucleus, μ^- decay endpoint is extended to the signal energy (105 MeV/c).
- Need a straw tracker with good momentum resolution, $< 200 \text{ keV/c}$ to distinguish DIO tail from signal.



Michel e^- ($< 52 \text{ MeV/c}$)

Signal (105 MeV/c)

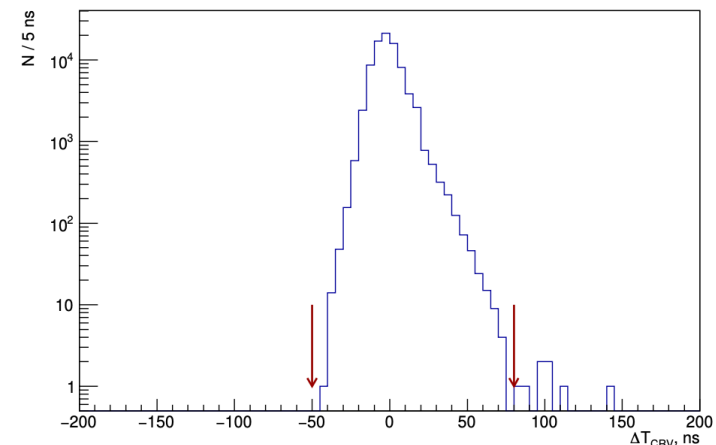
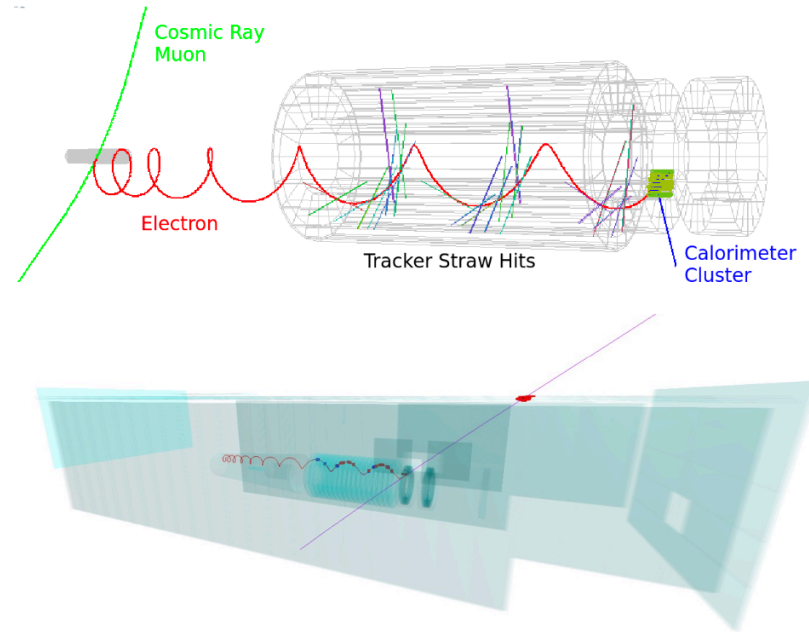
Problematic DIO tail ($> 100 \text{ MeV/c}$)



Background processes to $\mu^- \rightarrow e^-$ search

Cosmic rays

- Cosmic rays interacting with the detector material can produce signal-like e^-/e^+ .
- We expect ~ 1 signal-like event per day.
- Cosmic ray events are identified by having a coincidence cluster in the CRV with hits in 3/4 layers.
- The time of the reconstructed track matched to the CRV cluster is required to be within $-50 < t_{CRV} < 80$ ns of the cluster time.



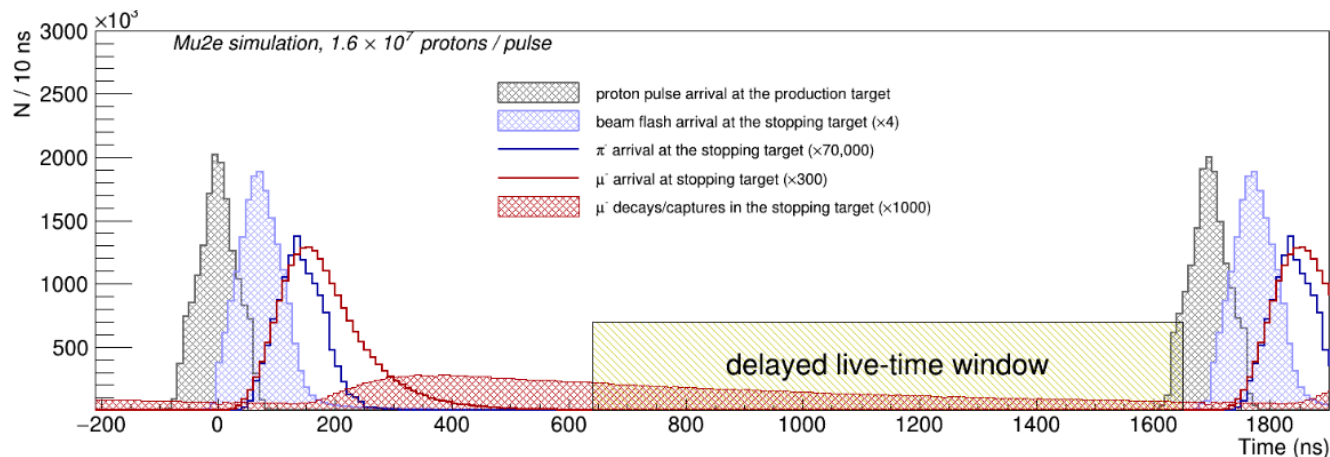
Background processes to $\mu^- \rightarrow e^-$ search

Radiative Pion Capture

- Pions contaminating the beam can survive to the stopping target, where radiative pion captures can produce signal-like e^-/e^+ .

$$\pi^- + N(A, Z) \rightarrow \gamma^{(*)} + N(A, Z - 1) \text{ followed by } \gamma^{(*)} \rightarrow e^+ + e^-.$$

- Pion lifetime 26 ns at rest. Pulsed proton beam (250 ns wide, pulses are 1695 ns apart). We can wait out the pion decay.
- In addition, upstream extinction removes out-of-time protons.



Background summary

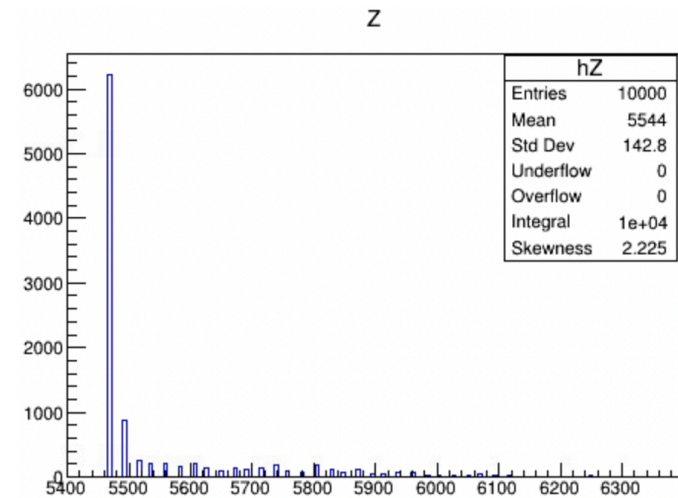
Channel	Mu2e Run I
Cosmic rays	$0.046 \pm 0.010(stat) \pm 0.009(syst)$
Decay in Orbit	$0.038 \pm 0.002(stat)_{-0.015}^{+0.025}(syst)$
Antiprotons	$0.010 \pm 0.003(stat) \pm 0.010(syst)$
RPC in-time	$0.010 \pm 0.002(stat)_{-0.003}^{+0.001}(syst)$
RPC out-of-time	$(1.2 \pm 0.1(stat)_{-0.3}^{+0.1}(syst)) \times 10^{-3}$
Radiative Muon Capture	$< 2.4 \times 10^{-3}$
Decays in flight	$< 2 \times 10^{-3}$
Beam electrons	$< 1 \times 10^{-3}$
Total	0.105 ± 0.032

Background summary using the optimised signal momentum and time window
 $103.6 < p < 104.90$ MeV/c and $640 < T_0 < 1650$ ns*

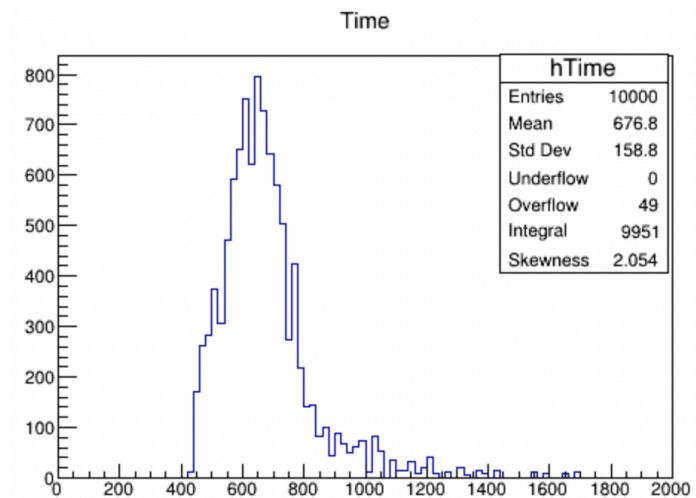
Background processes to $\mu^- \rightarrow e^-$ search

Antiprotons

- \bar{p} s are produced by the pW interactions in the Production Solenoid.
- Relatively low background but high systematic uncertainty.
- $p\bar{p}$ annihilation at ST can produce e^- s by $\pi^0 \rightarrow \gamma\gamma$ decays followed by the photon conversions and $\pi^- \rightarrow \mu^- \bar{\nu}$ decays followed by the μ^- decays.
- Can also cause delayed RPC.
- Background induced by \bar{p} cannot be efficiently suppressed by time window cut used to reduce prompt background.
- Absorber elements at entrance and centre of the Transport Solenoid to suppress the \bar{p} background.



**z (mm) from the centre of the TS
Longitudinal position of \bar{p} annihilations**



**time (ns) of \bar{p} annihilations
 \bar{p} s stop within the live data taking window**

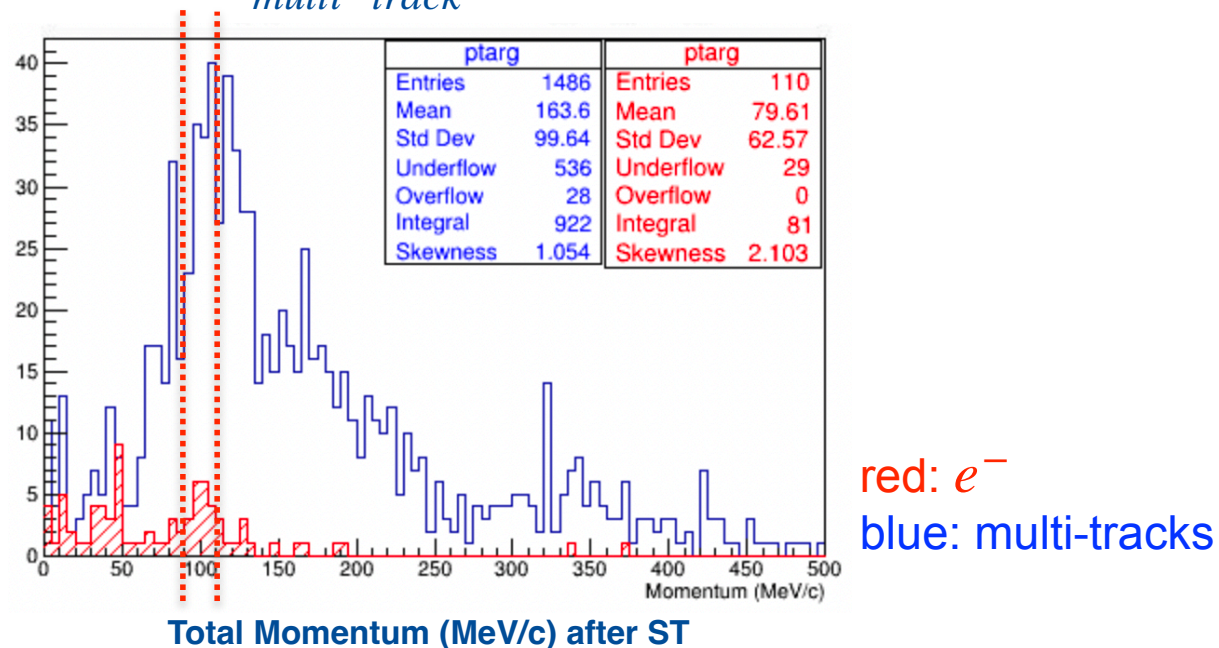
Estimating the \bar{p} background in Mu2e

- Background expected from \bar{p} is very low but highly uncertain due to the uncertainty in the \bar{p} production cross-section for the Mu2e proton beam energy and phase-space.
- We can exploit another final state with a much larger Branching Ratio to constrain the background by comparison.
- $p\bar{p}$ annihilation in the ST can give multiple tracks final state with $p \sim 100$ MeV/c for each track at a much higher rate than signal like e^- .

Estimating the \bar{p} background

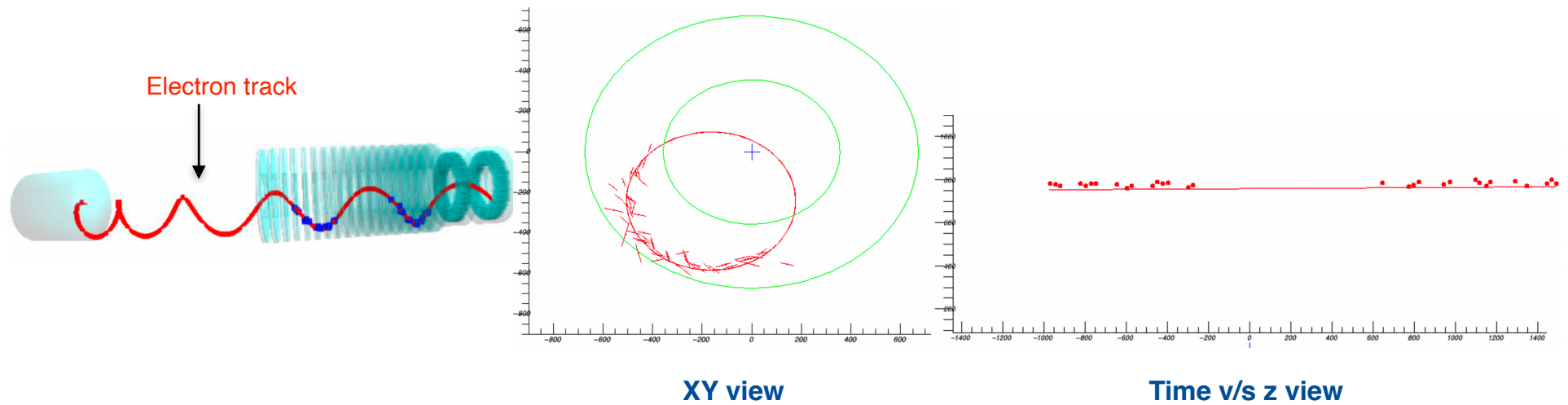
- In 10^4 $p\bar{p}$ annihilation events, only about **20** of the events contain **single electrons** with ≥ 20 straw hits and momentum in the range of 90-110 MeV/c.
- About 480 of the events contain **≥ 2 particles** with ≥ 20 straw hits per particle.

$$\frac{N_{e^- \text{ per MeV}}}{N_{\text{multi-track}}} \approx \frac{1}{500}$$

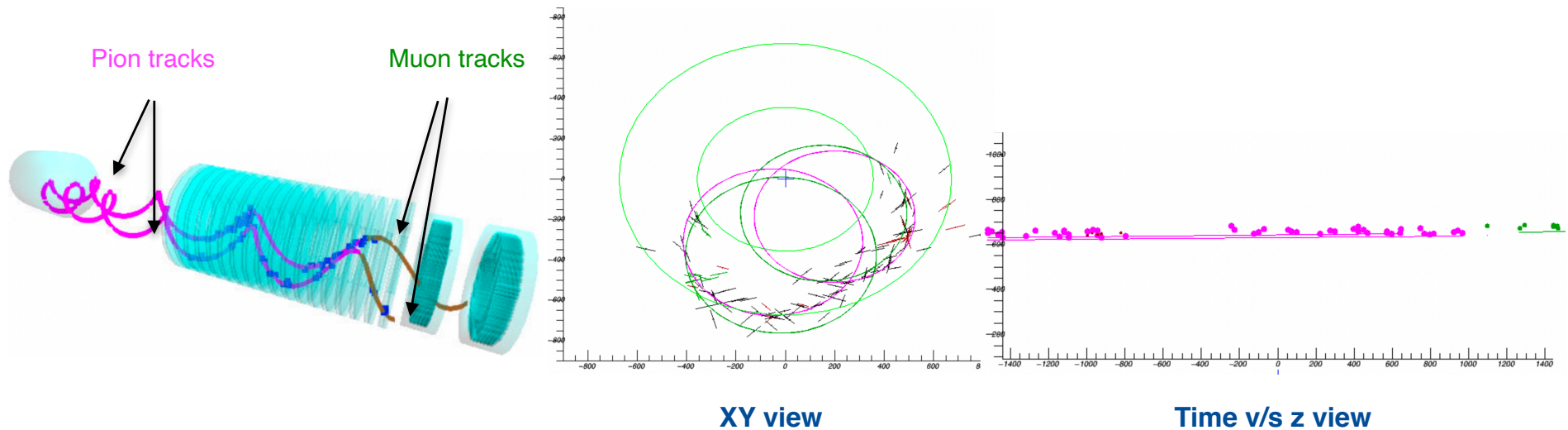


Goal: Identify and reconstruct the multi-track final state events and get an estimate of the CE like events by rescaling the ratio of the two final states.

Single interaction $p\bar{p}$ annihilation events in the Mu2e detector



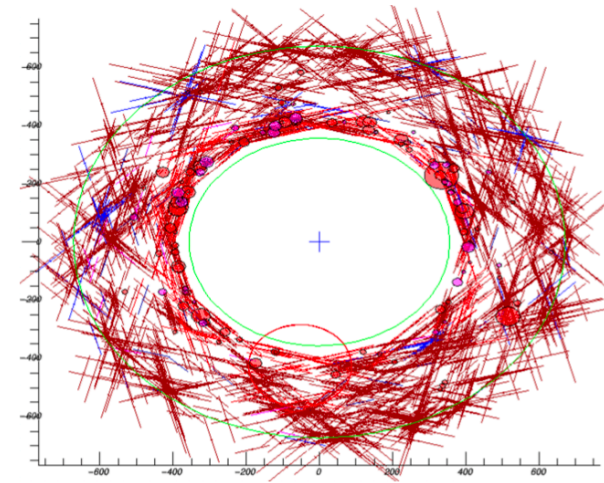
Events from $p\bar{p}$ annihilation in the ST. Red = electron, Green = Muon, Pink = Pion



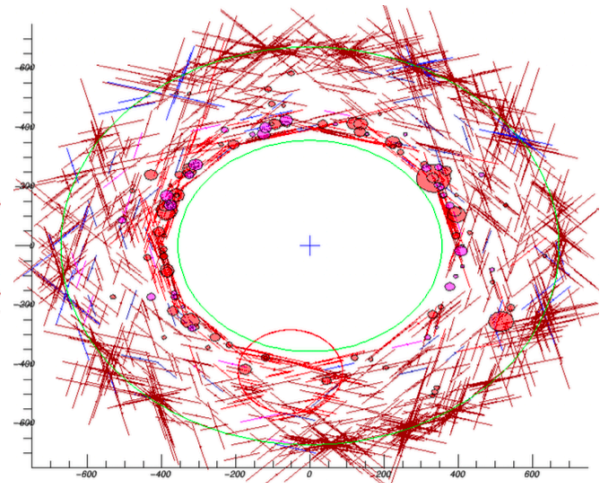
Goal: Identify and reconstruct the multi-track final state events and get an estimate of the **CE like** events by rescaling the ratio of the two final states.

A quick introduction to Mu2e event reconstruction

- Mu2e event reconstruction is optimised to reconstruct single-track events with tracks coming from the ST.
- From MC, $> 90\%$ of the hits in an event are from low energy e^-/e^+ and protons. They have to be flagged as background prior to the track reconstruction.
- We cluster the hits within a time window to form *TimeClusters* assuming that such hits are made by the same particle.
- Hits from *TimeClusters* are used to form helices.
- Final parameters of the track are determined by the Kalman fit.



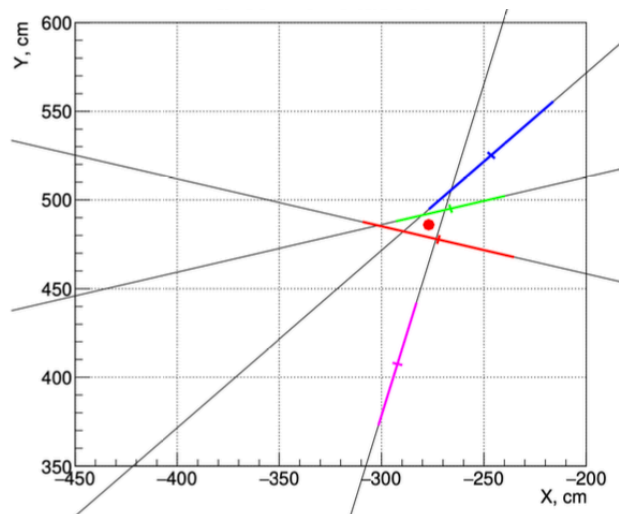
An event before background hits flagging
Blue: e^+ Maroon: e^-



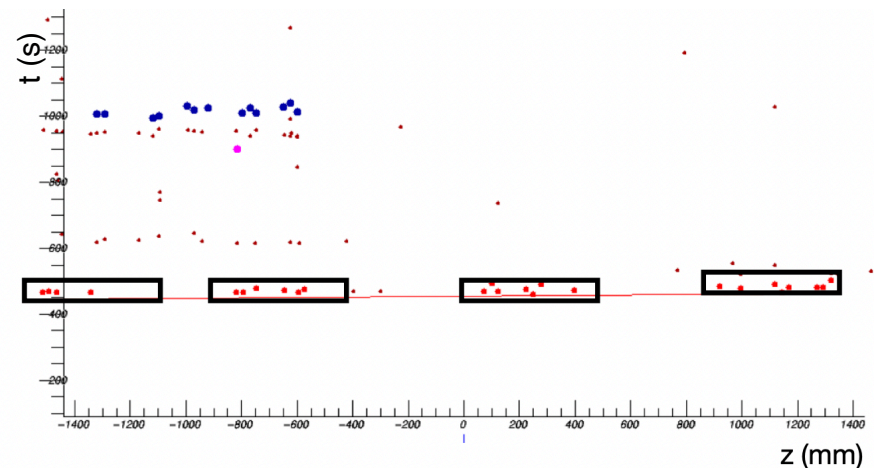
An event after background hits flagging

Background hit flagging and Time Clustering

- Current standard algorithms to remove low energy e^-/e^+ hits and time clustering have an ANN layer trained for efficient signal e^- identification and reconstruction. They inadvertently remove a significant fraction of hits from the pion and muon tracks.
- More physics neutral algorithms, highly efficient for a wide spectrum of particle topologies were developed to remove the low energy background hits and time clustering.
- The new time clustering performs a 2-D search using the time and z information of the hits to form *TimeClusters*.
- With the new algorithms the rejection factor of pions and muons has been significantly reduced.



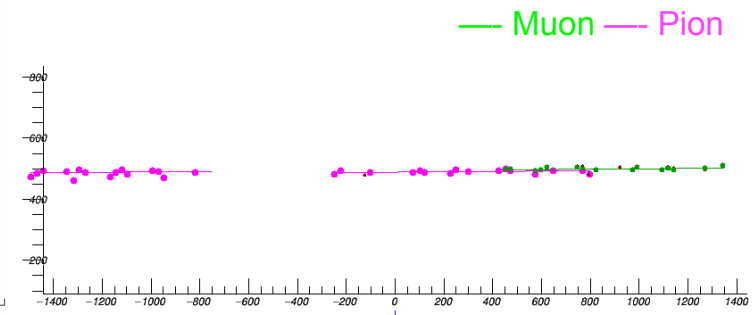
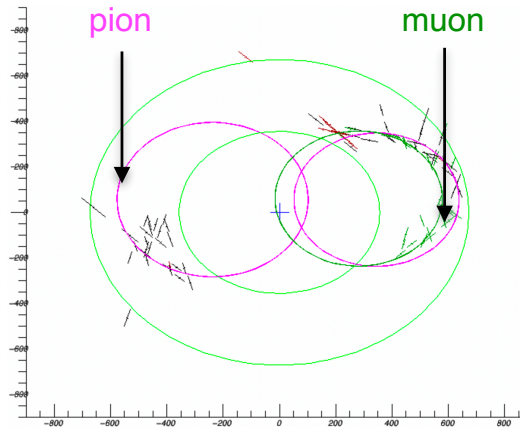
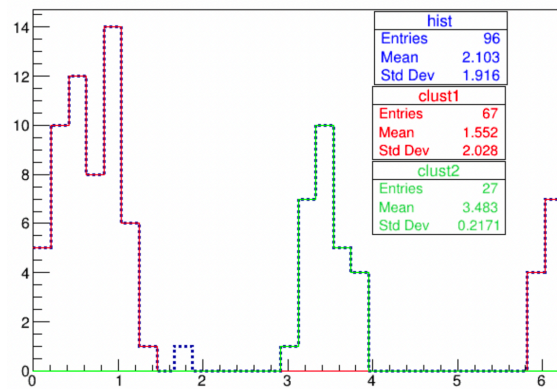
A δe^- candidate seed. The 4 segments are the tracker straws that were hit in one station and form a stereo hit.



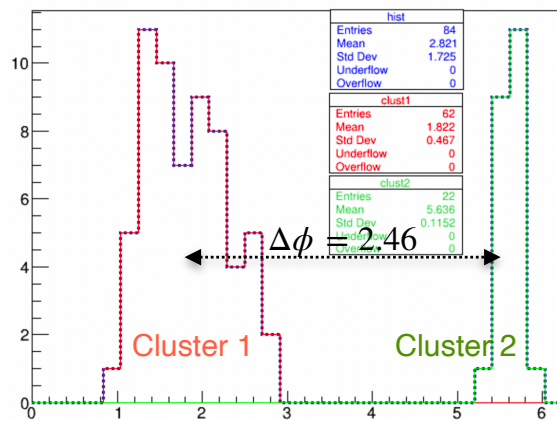
Time v/s z view of the hits in a CE + 1BB pileup event

Early Stage Hit Phi Clustering

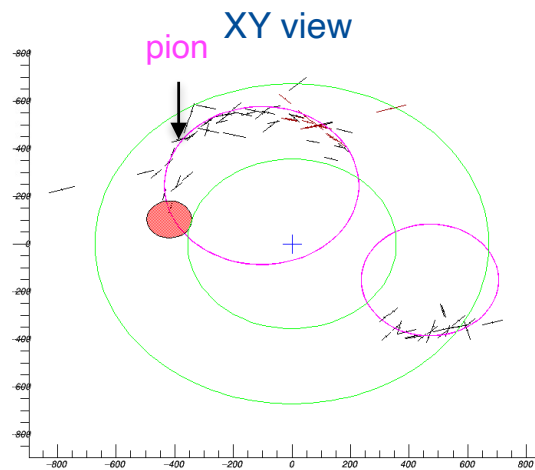
- Hits from different particles in the same time window could be well separated in ϕ or overlapping. We began with the simple case of well separated tracks.
- We developed a ϕ clustering algorithm to group hits of a time cluster based on their ϕ distribution.



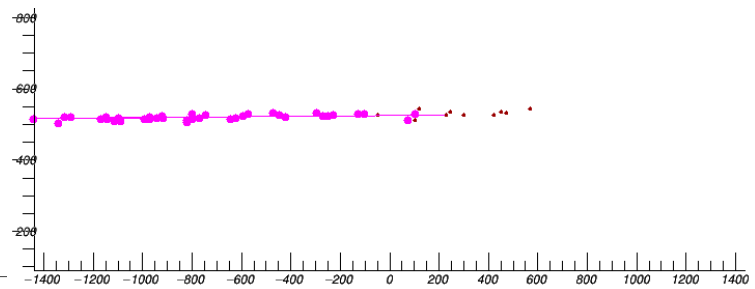
$\Delta\phi = 2.96$ rad



$\Delta\phi = 2.46$ rad



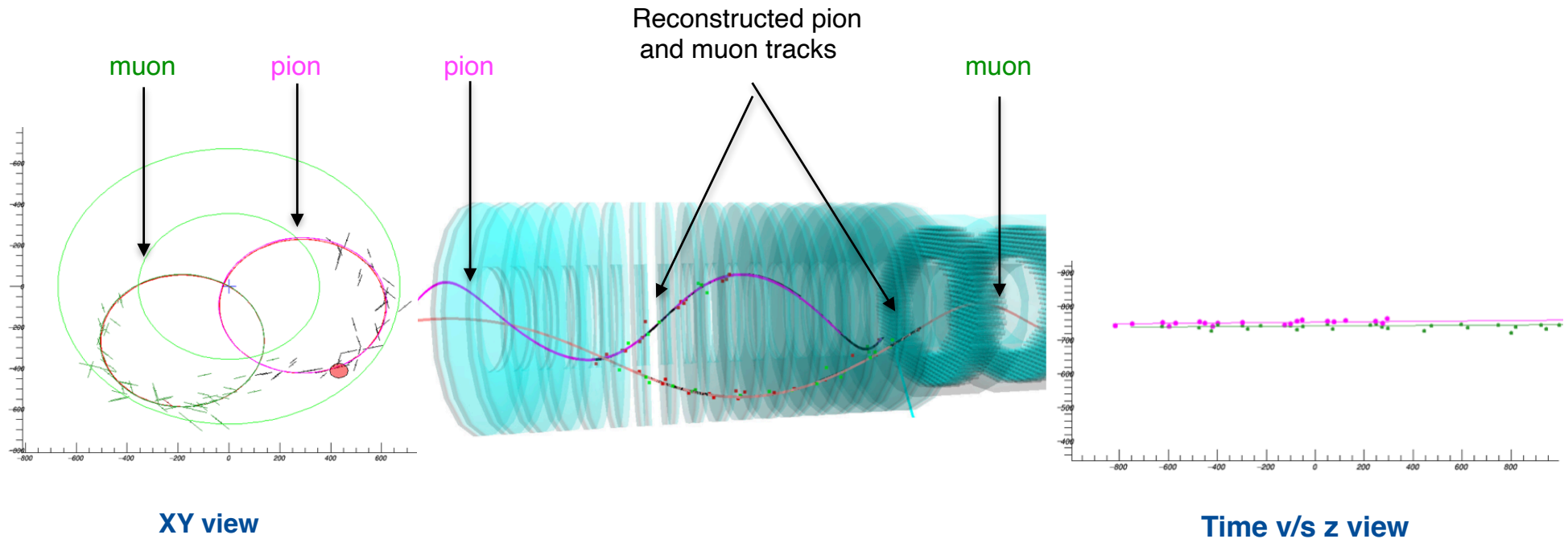
Time v/s z view



XY view

Time v/s z view

Preliminary results (single interaction $p\bar{p}$ annihilation events)

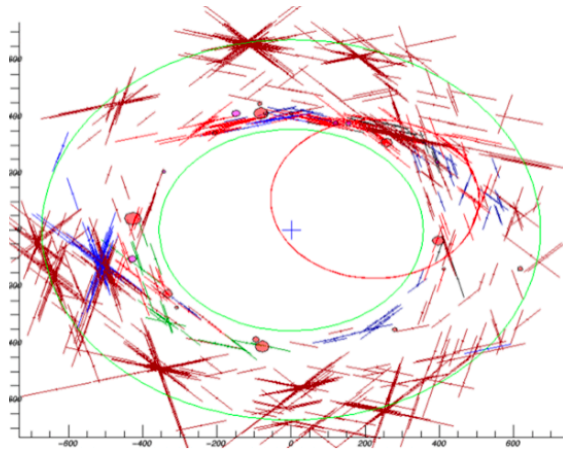


A $p\bar{p}$ annihilation at the ST event with two reconstructed tracks

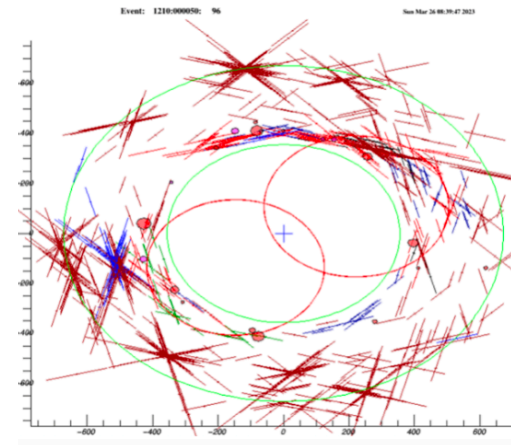
Green = Muon, Pink = Pion, Black = Reconstructed track in 3-D view
Red = Reconstructed track in 2-D views

Results

- Generated 10^4 $p\bar{p}$ annihilation + 1BB and 2BB pileup data samples respectively.
- Tested and compared the performance of the new algorithms (*DeltaFinder**, *TZClusterFinder*** and the ϕ *ClusterFinder*) with the default Offline reconstruction.



XY view, Default reconstruction



XY view, New reconstruction

Dataset	0 BB		1 BB		2 BB	
	> 0 track	> 1 track	> 0 track	> 1 track	> 0 track	> 1 track
Default reco	1272	58	1089	46	1046	39
New reco	1734	113	1579	97	1465	81
Improvement	x 1.4	x 2	x 1.4	x 2.1	x 1.4	x 2

**Contribution of other backgrounds
to
the multi-track events signature**

DIO

- For Run I, about 75% of the total protons on target (POT) will be delivered with mean intensity of 1.6×10^7 protons/pulse and 25% in the high intensity mode with 3.9×10^7 protons/pulse.
- The average number of stopped muons/POT is 1.6×10^{-3} .

Running Mode	Mean Proton Pulse Intensity	Running Time (s)	N (POT)	N (Stopped Muons)
Low intensity	1.6×10^7	9.5×10^6	2.9×10^{19}	4.6×10^{16}
High intensity	3.9×10^7	1.6×10^6	9.0×10^{18}	1.4×10^{16}
Total		11.1×10^6	3.8×10^{19}	6.0×10^{16}

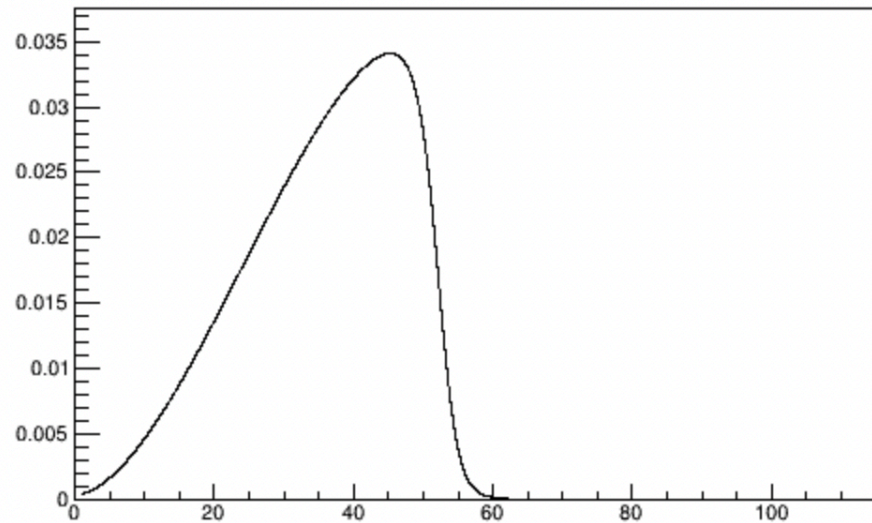
Expected running time, proton counts, and stopped muon counts for Mu2e Run I.

- 39% of stopped muons Decay in Orbit (DIO) $\Rightarrow \approx 10^4$ DIO per event. For the high intensity mode, the corresponding number is about 2.5 times higher.
- In Run I we can expect about 2.34×10^{16} total number of DIO electrons.

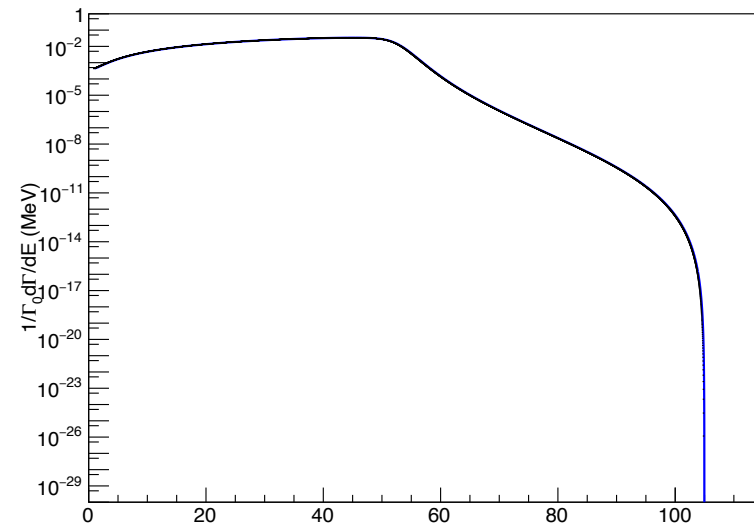
DIO

- We look for particle tracks with momentum > 90 MeV/c,
 $N_{DIO}(E > 90) = (7.3 \times 10^{-10}) \times (2.34 \times 10^{16})$
 $N_{DIO}(E > 90) = 1.7 \times 10^7$
- For the \bar{p} background estimation, we look for multiple particle tracks per event where each particle has a momentum > 90 MeV/c.

$$N_{2DIO}(E > 90) = 1.25 \times 10^{-2}$$



DIO e^- Energy (MeV) Linear scale



DIO e^- Energy (MeV) Log scale

* https://github.com/Mu2e/Offline/blob/main/ConditionsService/data/heck_finer_binning_2016_szafron.tbl

Contribution of DIO to multi-track events

- Assuming a track reconstruction efficiency of ~ 0.1 (from SU2020 studies)

$$N_{2RecoDIO}(E > 90) = 1.25 \times 10^{-2} \times 10^{-1} \times 10^{-1}$$

$$N_{2RecoDIO}(E > 90) \approx 10^{-4}$$

- Assuming a uniform DIO distribution in time and same efficiency of reconstruction for multi track events as single tracks:

$$N_{2RecoDIO}(E > 90, \Delta T < 100ns) \approx 10^{-5}$$

- Therefore, if one asks for the track to have at least 90 MeV/c momentum then the probability of a two DIO tracks event is negligible.

Cosmics Dataset

- The CRY4 Lo dataset (MDC2020Datasets) had a p_{max} cut at 500 MeV/c. The strip was CE-biased.
- The parent CRY Lo datasets are huge. Most of the events not particularly useful.
- Parent dataset: dts.mu2e.CosmicCRY.010722.art (Stage 2 Low)
File count: 90,685
Total size: 4T
Event count: 692,979,476
- Created a new filter module to generate a dataset manageable in size and useful for most studies like VST and Calibration studies as well.

If ($p \leq 1$ GeV/c and number of “hit” stations > 3 and NHits > 8), save the event.
Else if ($p > 1$ GeV/c and Nhits ≥ 8) save the event.

- **The new CRY lo dataset can be found:**

```
samweb list-files --summary "dh.dataset=dts.mu2e.cry4lb0s31r0000.pbar2m.art"  
File count: 1000  
Total size: 249751538458 (200GB)  
Event count: 18007806
```

Cosmics Dataset

- We generated the Cosmics (CRY Lo) + 1BB dataset as well.
- Faced some issues like the absence of SimEfficiency Table for Run 2701. Solved by creating a .txt file with the mixing efficiency numbers and pointed to it in the fcl file ([docdb.38507](#)).
- The mixed dataset would have been very large in size (30 TB). So, we applied tighter selection cuts:

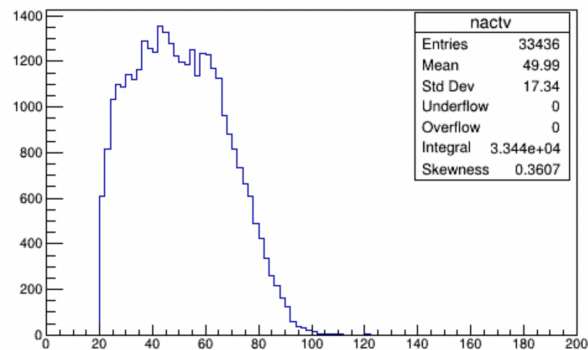
At least one particle must satisfy: $50 \leq p \leq 250 \text{ MeV}/c$, $N_{HitStations} \geq 4$, $N_{Digis} \geq 10$.

- **The 1BB mixed CRY4 Lo dataset can be found:**

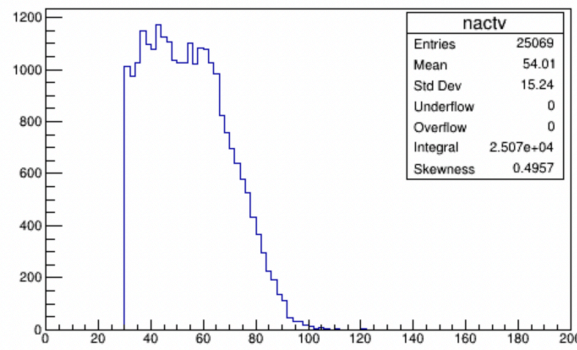
```
samweb list-files --summary "dh.dataset=dig.mu2e.cry4lb1s41r0000.pbar2m.art"  
File count:    498  
Total size:    1803711346022  
Event count:   1014574
```

Cosmics Dataset: An oversampling issue

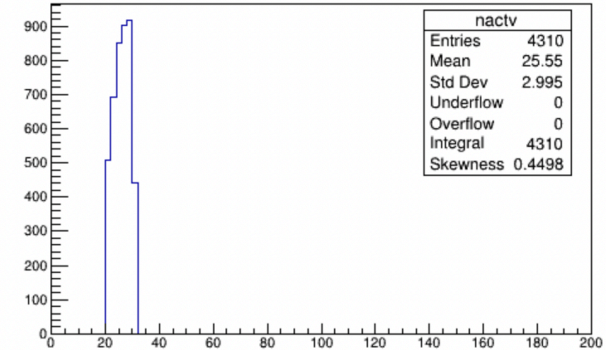
- Ran reconstruction on some of the Cosmics + 1BB digi files.
- Observed a bump in the 210-220 MeV/c momentum range of reconstructed tracks.
- We noticed that most of these tracks have $20 < n\text{Strawhits} < 30$.



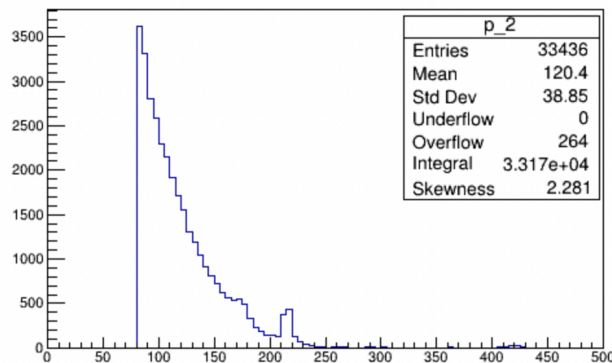
NHits > 20



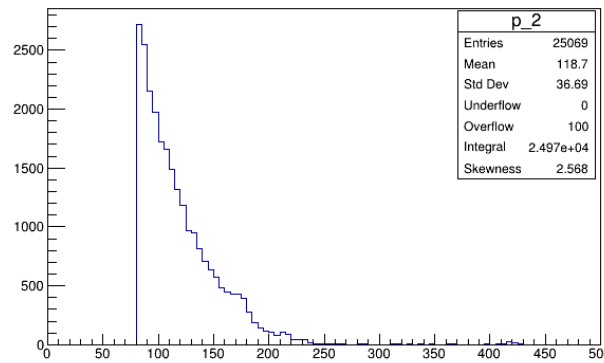
NHits > 30



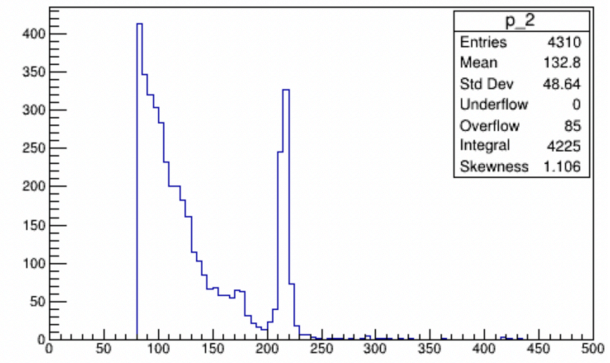
20 < NHits < 30



Momentum (Mev/c)



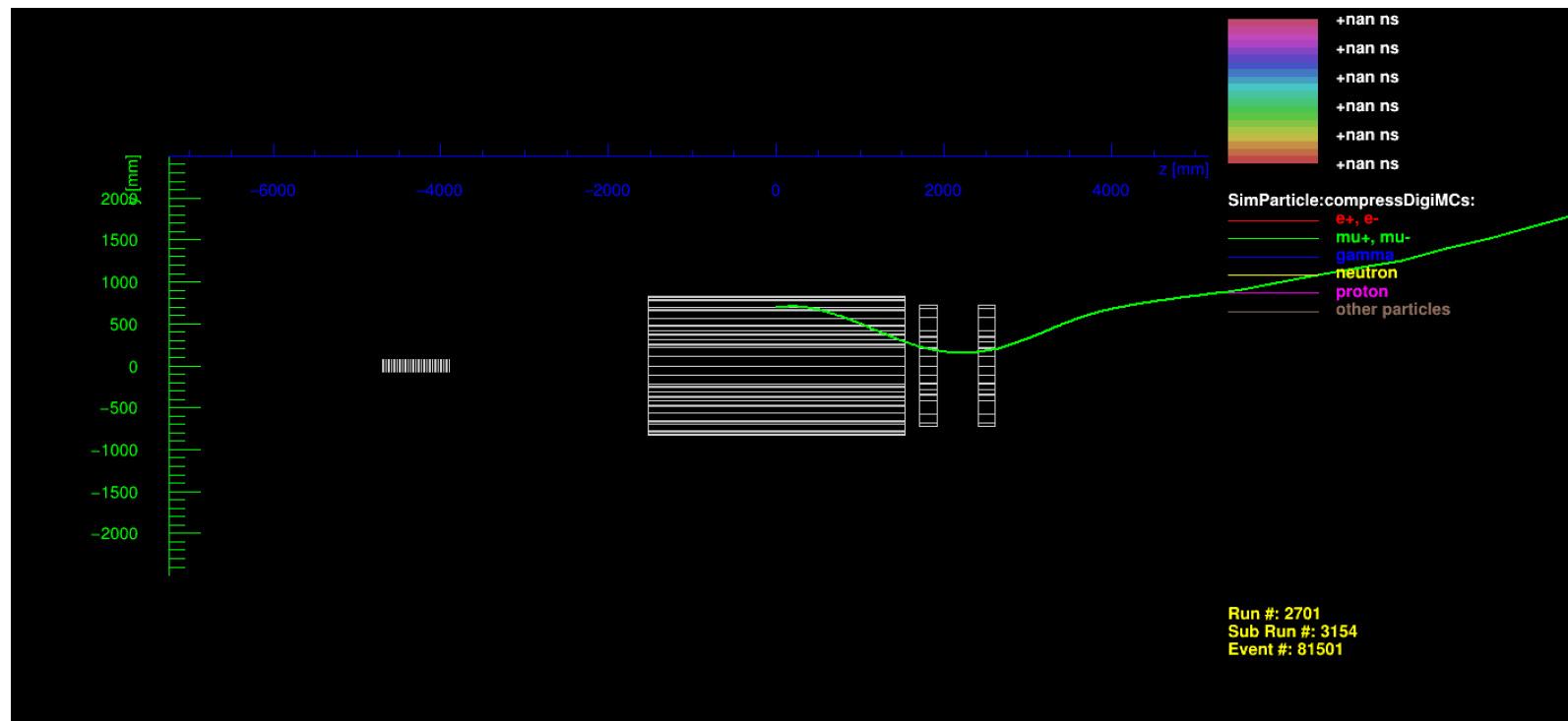
Momentum (Mev/c)



Momentum (Mev/c)

Cosmics Dataset: An oversampling issue

- This is an event with a cosmic muon entering from the back, not interacting with the Calorimeter and making about 20-30 hits in the Tracker.
- Such an event occurs about 30-50 times every ~ 15000 events or so.



Courtesy: Y. Oksuzian

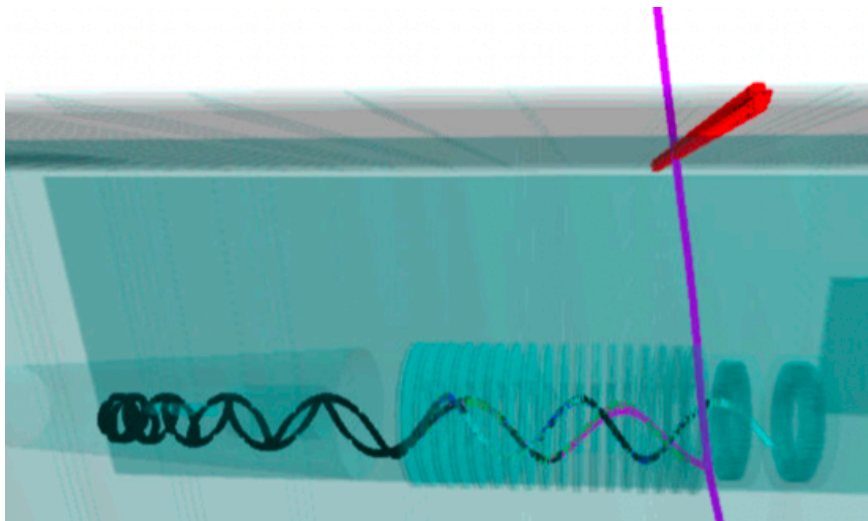
Multi-track events from Cosmics

- Most of the Cosmics multi-track events are:

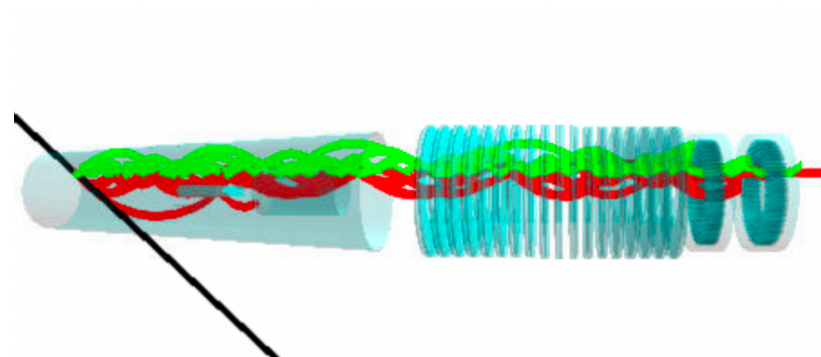
(1) Cosmic muons interacting with the calorimeter disk, producing an e^+/e^- which first travels upstream towards the ST and then returns back.

(2) Cosmic muons interacting with the ST, producing e^+ 's and e^- 's.

- Thus, most cosmic multi-track events are made of an upstream and downstream moving leg of the same particle while \bar{p} annihilation at the ST gives multiple particle tracks moving downstream from the ST.



(1)



(2)

CRV Reconstruction

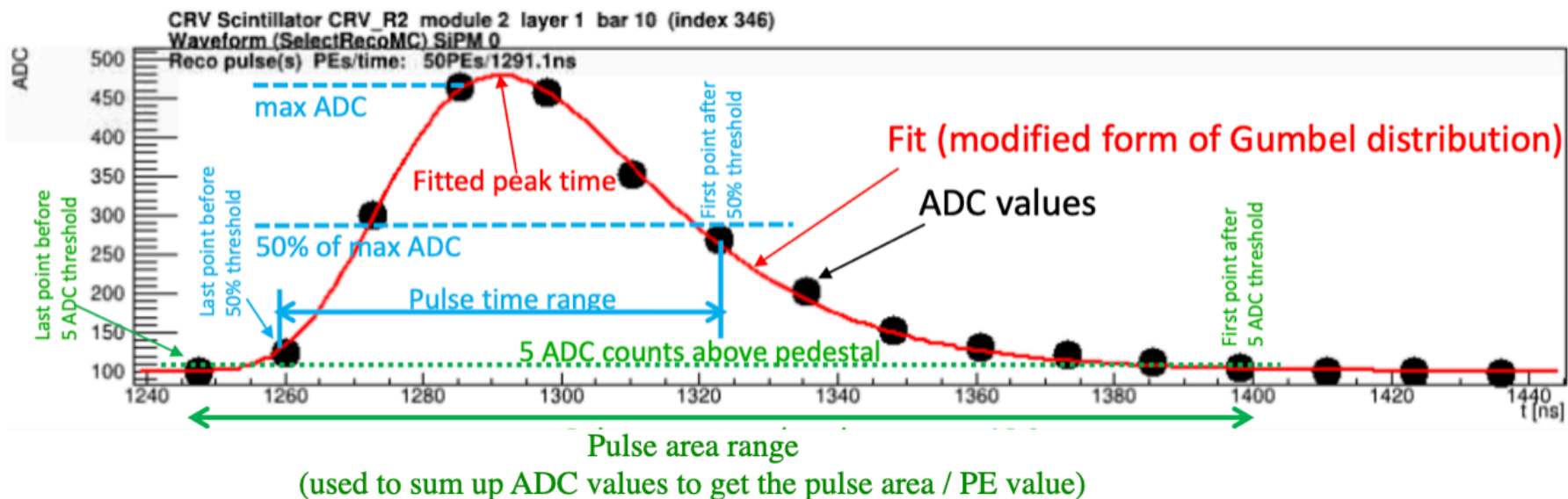
- CRV pulse reconstruction

(1) Using a modified form of Gumbel function ($f(x) = e^{-x+e^{-x}}$) for fit. The peak time, peak height and the pulse area of the CRV pulse are obtained from the fit.

$$ADC(t) = A \cdot e^{-\left(\frac{t-\mu}{\beta}\right) - e^{-\left(\frac{t-\mu}{\beta}\right)}}$$

where the pulse height = A/e , peak time = μ and the pulse area = $A \cdot \beta$.

(2) Without a fit : The pulse start/end time are based on the time the waveform crosses a threshold. The pulse area is based on the sum of the (pedestal-subtracted) ADC values.



CRV Reconstruction

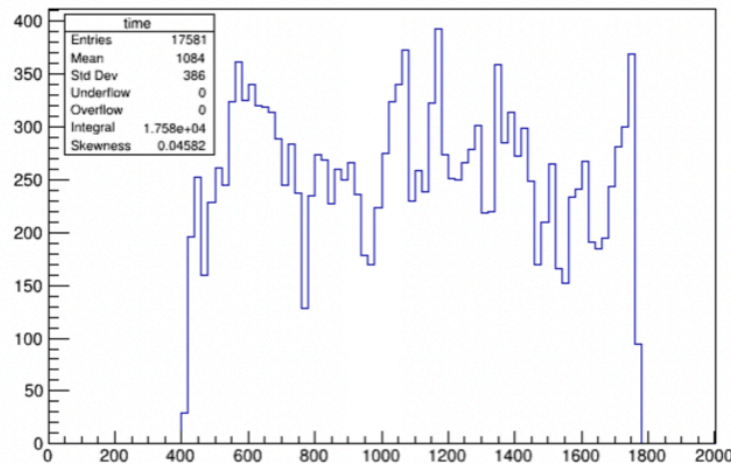
- Next, we find *Coincidence groups*, a group of CRV pulses that satisfy the following criteria:
 - > Hits must be on the same readout side.
 - > Group of hits must satisfy a minimum number of layers.
 - > Pulses must satisfy a minimum number of PEs per individual pulse (or neighbouring pulses, if they occur with a certain time) requirement.
 - > **Pulses must satisfy the minimum overlap time/maximum time difference between them.**
 - > There is a minimum/maximum slope between two pulses in different layers and maximum slope variation between different pulse combinations requirement.
 - > For all the above mentioned parameters, each CRV sector can have a different criteria/threshold.

CRV Reconstruction

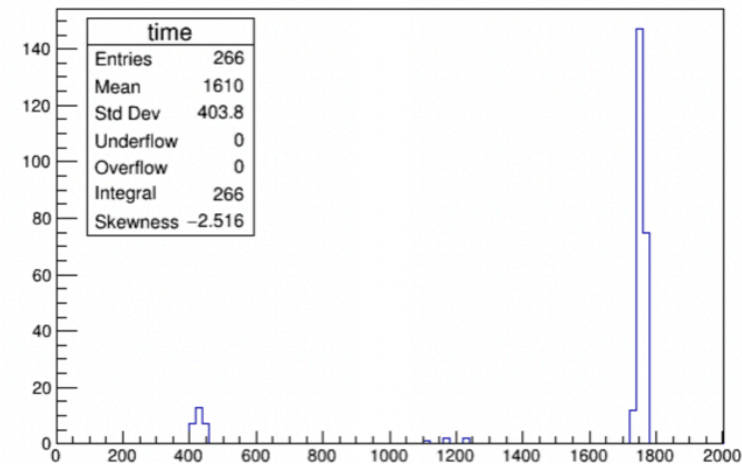
- Coincidence groups that occur close in time and distance to each other are merged into CRV Coincidence Clusters.
- Following are the criteria to form a CRV Coincidence Clusters:
 - (1) Only coincidence groups that are in the same CRV sector type are merged together, regardless of the readout side.
 - (2) Certain parameters of the clusters are calculated like the total number of PEs, start/end time of the cluster and PE-weighted average position of the cluster and slope and they must satisfy the minimum requirements.
- More details can be found at <https://mu2e-docdb.fnal.gov/cgi-bin/sso/ShowDocument?docid=46499>, <https://mu2e-docdb.fnal.gov/cgi-bin/sso/ShowDocument?docid=44722> (R.Ehrlich).

Scope for improvement

- Contrary to what we had expected to observe in the *CRYhigh* dataset, we found about 20% of the events with no CRV Coincidence Clusters.
- Most of these events with no coincidence cluster occur either before 450 ns or after 1700 ns, close to the edge of the microbunch/OnSpill event window. **The CRV pulses fail the minimum time overlap criteria** required to form a coincidence cluster as they are all assigned the exact same timing value at the start and end of the microbunch.
- In about 80% these events there are no reconstructed CRV pulses at all because the waveform is abruptly cut towards the end and the pulse fails the fit.



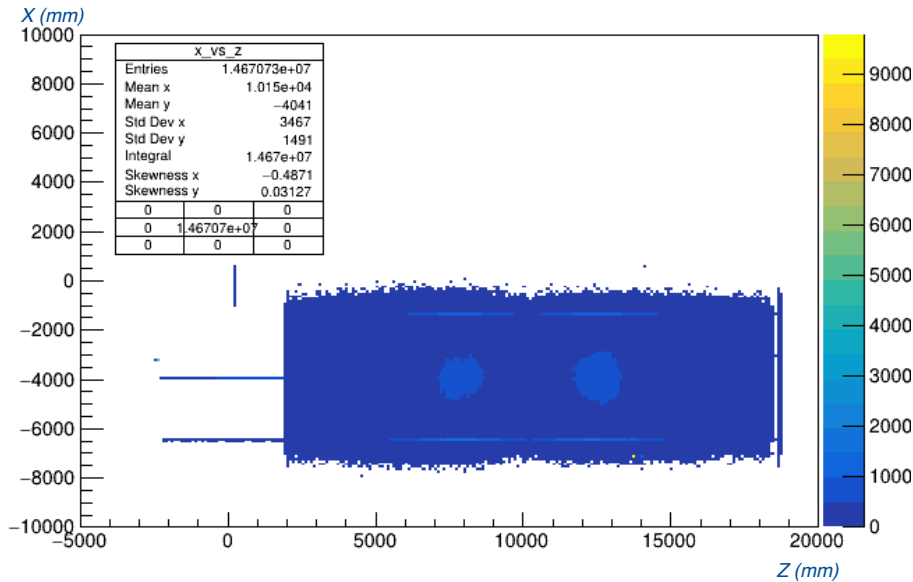
CRV Pulse time (ns)
All events



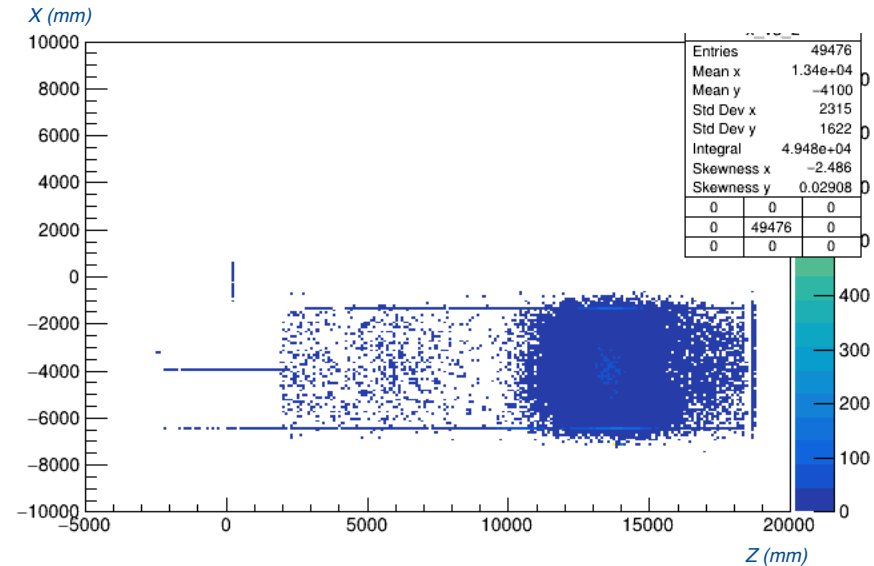
CRV Pulse time (ns)
Events with no CRV Coincidence clusters

Multi-track events from Cosmics

- Most multi-track cosmic ray events are made of an upstream and downstream moving leg of the same particle while \bar{p} annihilation at the ST gives multiple particle tracks moving downstream from the ST.



Events with ≥ 1 reconstructed track



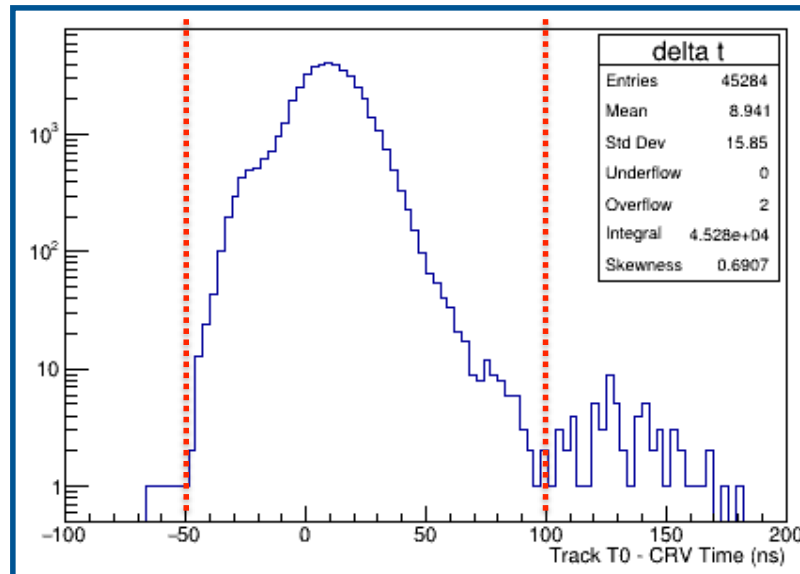
Events with ≥ 2 reconstructed track

x vs z distribution of the CRV Coincidence Clusters.

Multi-track events from Cosmics

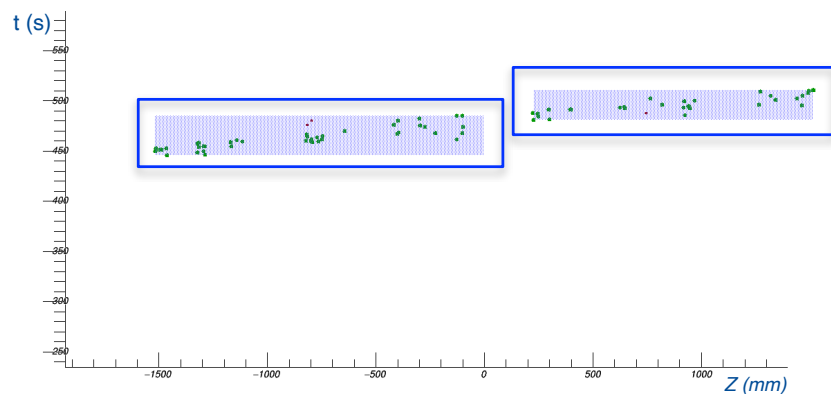
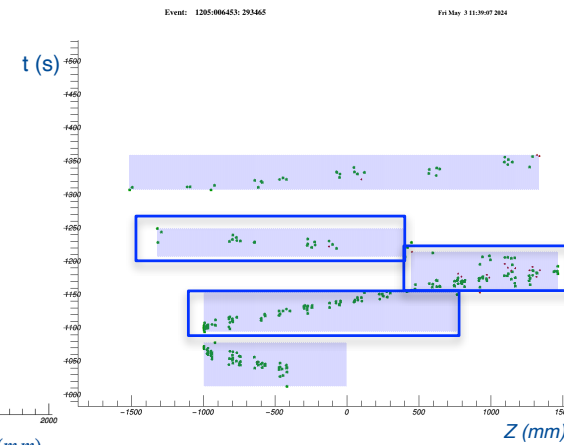
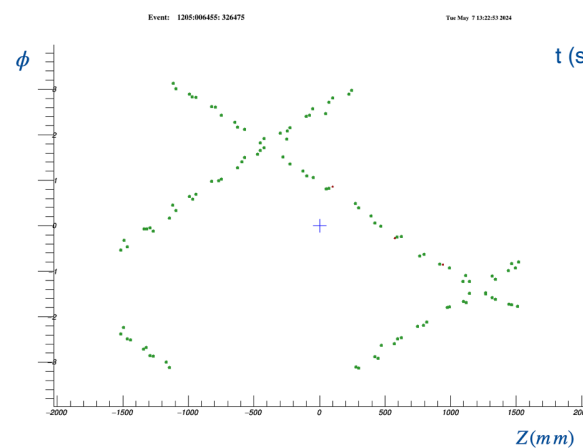
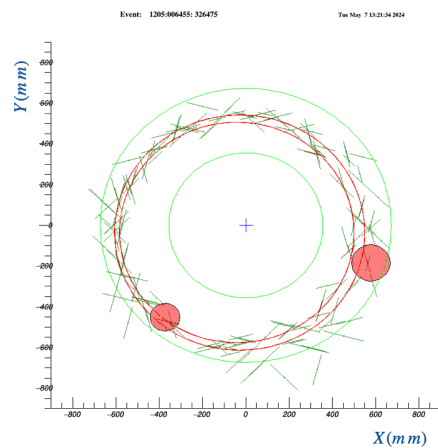
- About 99.98% of these multi-track events can be vetoed using the signal from the CRV.

Cosmic event candidates are identified by the timing window $-50 < \Delta T_{CRV} < 80ns$ where $\Delta T_{CRV} = T_0 - T_{CRV}$.



Scope for improvement in reconstruction

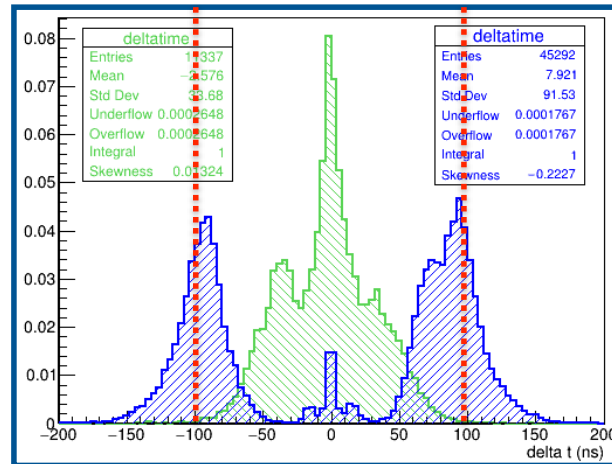
- We faced an issue of split time clusters. It led to the non veto of some cosmic ray events as $\Delta T_{CRV} > 100$ ns, which was not true in reality.



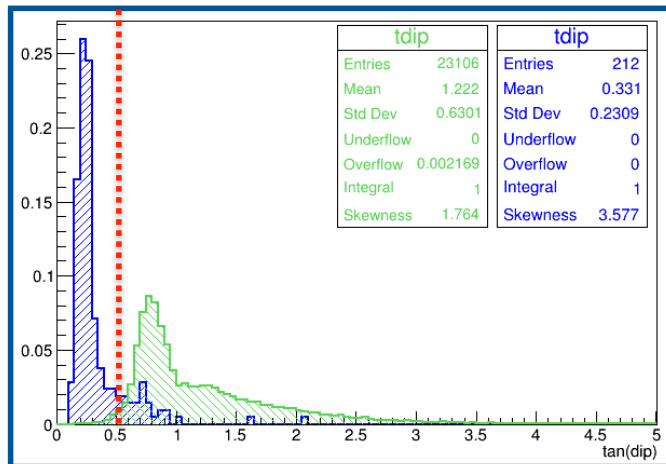
<https://github.com/Mu2e/pbar2m/issues/5>

Multi-track events from Cosmics

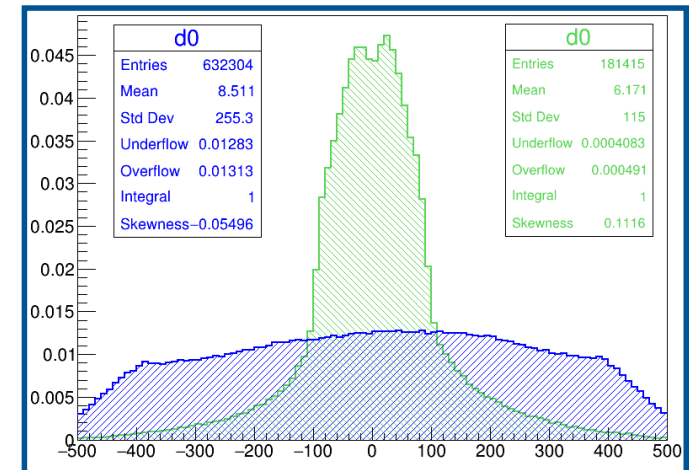
- For events with no matched CRV signal, we have identified track parameters: pitch($\tan(\lambda)$), impact parameter ($D0$) that can be used to distinguish tracks from cosmic muons from $p\bar{p}$ background events.



Blue: cosmic rays
Green: tracks from $p\bar{p}$ annihilation at ST



$$\Delta T_{\text{trk}}(\text{ns})$$



$\tan(\lambda)$

$D0$ (mm)

Multi-track events from Cosmics

- The topology of a multi-track event from cosmic rays is quite different from the multi-track event signature expected from $p\bar{p}$ annihilation at the ST in Mu2e.
- We can veto most of the cosmic ray interactions using the CRV stub and reconstructed track time. The rest can be vetoed using the track parameters like pitch ($\tan(\lambda)$), impact parameter ($D0$), ΔT_{trk} with minimal loss to the \bar{p} background events.
- We have identified a number of issues with the present reconstruction algorithms like the following:
 - (1) In several events, at the time clustering stage, hits of a single particle trajectory, close in time and z are split into two time clusters.
 - (2) The upstream track reconstruction fails in many events as well. For many of these tracks, the helix is reconstructed but with less than 25-30 straw hits associated with the helix, while their parent time cluster has a large number of hits in the cluster.

Systematic Uncertainties I: Pion Multiplicity

$\bar{p}N$ annihilation

- First of, we deal with $\bar{p}N$ annihilation (Al target) at rest and not just $p\bar{p}$ annihilation.
- \bar{p} annihilation at rest in different nuclei is not well studied.
- 1955-56: A program to detect and study \bar{p} s in emulsions was initiated concurrently with the counter experiment at the Berkeley Bevatron that demonstrated the existence of \bar{p} s.
- 1960s: Detailed studies of $p\bar{p}$ annihilation at rest were carried out using bubble chambers at BNL and CERN.
- 1983-96: Low Energy Antiproton Ring (LEAR) at CERN. Around 15 experiments studying annihilation. Most important ones are ASTERIX, OBELIX and CRYSTAL BARREL.
- Asterix collaboration investigated annihilation from P-states of the $p\bar{p}$ atom formed in H_2 gas with a 2π electronic detector.
- Crystal-Barrel research was focused on annihilation at rest and in flight. Obelix investigated \bar{p} and \bar{n} interactions at rest and with very low momenta. They both used 4π spectrometers.

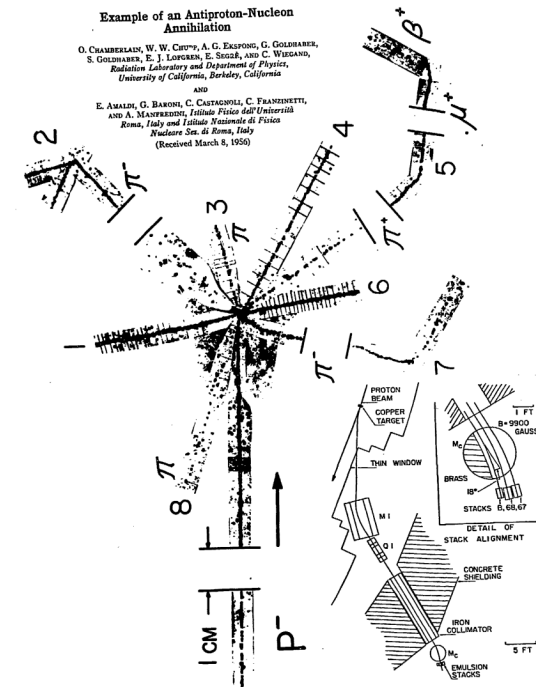
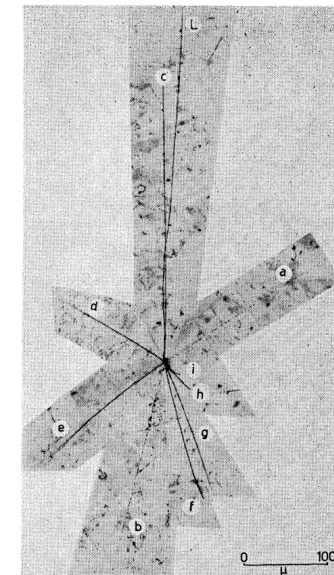


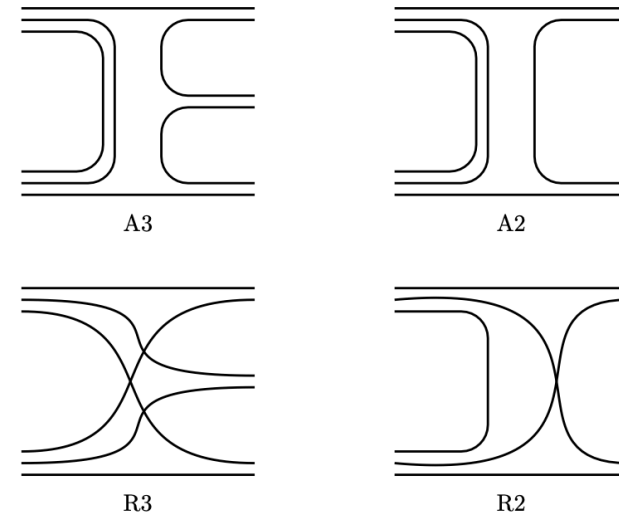
Fig. 6 Photo micrograph of first event found by "along the track" scanning in the second exposure. This event, which released 1300 ± 50 MeV of visible energy gave the conclusive proof for the annihilation process.



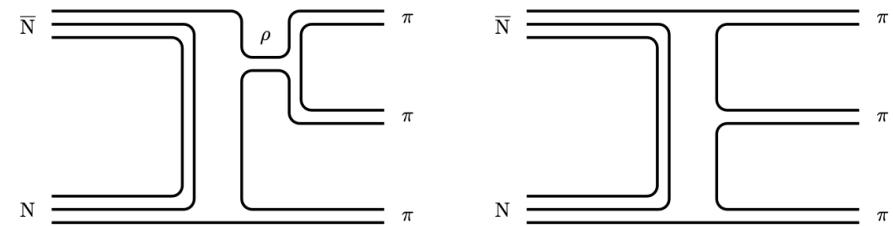
INFN, Rome 1955-56

The quark model

- Annihilation is a fascinating process, in which matter undergoes a transition from its baryon structure to one consisting solely of mesons.
- An average of five pions are produced in $N\bar{N}$ annihilation at rest.
- In baryon-exchange picture or in quark models, a few meson resonances are primarily produced, the observed final states resulting from the decay of these resonances.
- The quark model explains why a baryon and its antiparticle can energetically annihilate by simple rearrangement, $(\bar{q}\bar{q}\bar{q}) + (qqq) \rightarrow (\bar{q}q) + (\bar{q}q) + (\bar{q}q)$, at rest.
- Considering the quark model, $p\bar{p}$ annihilation can at most give 1 π^+ , 1 π^- and 1 π^0 . While $\bar{p}n$ annihilation can give at most 1 π^+ and 2 π^- .
- Therefore, in $p\bar{p}$ annihilations equal number of π^+ and π^- are produced and in $\bar{p}n$ annihilations the number of π^- exceeds that of π^+ by 1.



Annihilation (A2, A3) and rearrangement (R2,R3) diagrams for $N\bar{N}$ annihilation.



Possible mechanisms for $\pi\pi\pi$ production.

Isospin conservation

- Strong interactions obey the conservation laws: energy E , momentum p , angular momentum J , parity P and charge conjugation C , as well as flavours.
- Isospin and G-parity are also conserved. G-parity is a combination of charge conjugation and isospin, $G = C \exp(-i\pi I_2)$.
- Proton and neutron form an isospin doublet and so do the up and the down quark.
- The $\bar{p}n$ system is in a pure isospin state with $I = 1$ and the $p\bar{p}$ system is in a mixture of states with $I = 1$ and $I = 0$.

$$|p\bar{p}\rangle = \frac{|I = 1\rangle - |I = 0\rangle}{\sqrt{2}}$$

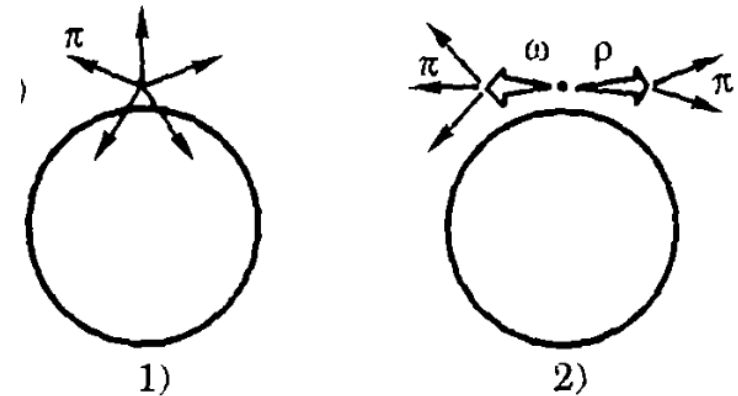
- If n_+ is the average number of π^+ , etc., with the obvious relation $n_+ + n_- + n_0 = n_\pi$ an $I = 0$ initial state, which is isotropic in isospin space, will lead to $n_+ = n_- = n_0 = n_\pi/3$. For $I = 1$ initial state, look at the back-up slides.

L	S	J	n	$I = 1$	$I = 1/2$	$I = 0$	$I = 0$	J^{PC}	$n^{2s+1}L_J$
0	0	0	1	π	K	η	η'	0^{-+}	1^1S_0
0	1	1	1	ρ	K^*	ϕ	ω	1^{--}	1^3S_1
1	0	1	1	$b_1(1235)$	K_{1B}	$h_1(1380)$	$h_1(1170)$	1^{+-}	1^1P_1
1	1	0	1	$a_0(1450)$	$K_0^*(1430)$	$f_0(1710)$	$f_0(1370)$	0^{++}	1^3P_0
1	1	1	1	$a_1(1260)$	K_{1A}	$f_1(1420)$	$f_1(1285)$	1^{++}	1^3P_1
1	1	2	1	$a_2(1320)$	$K_2^*(1430)$	$f_2(1525)$	$f_2(1270)$	2^{++}	1^3P_2
2	0	2	1	$\pi_2(1670)$	$K_2(1770)$	$\eta_2(1870)$	$\eta_2(1645)$	2^{-+}	1^1D_2
2	1	1	1	$\rho(1700)$	$K^*(1680)$	$\phi(????)$	$\omega(1650)$	1^{--}	1^3D_1
2	1	2	1	$\rho_2(????)$	$K_2(1820)$	$\phi_2(????)$	$\omega_2(????)$	2^{--}	1^3D_2
2	1	3	1	$\rho_3(1690)$	$K_3^*(1780)$	$\phi_3(1850)$	$\omega_3(1670)$	3^{--}	1^3D_3
0	0	0	2	$\pi(1370)$	K(1460)	$\eta(1440)$	$\eta(1295)$	0^{-+}	2^1S_0
0	1	1	2	$\rho(1450)$	$K^*(1410)$	$\phi(1680)$	$\omega(1420)$	1^{--}	2^3S_1

Possible mesons from \bar{p} annihilation

Annihilation radius

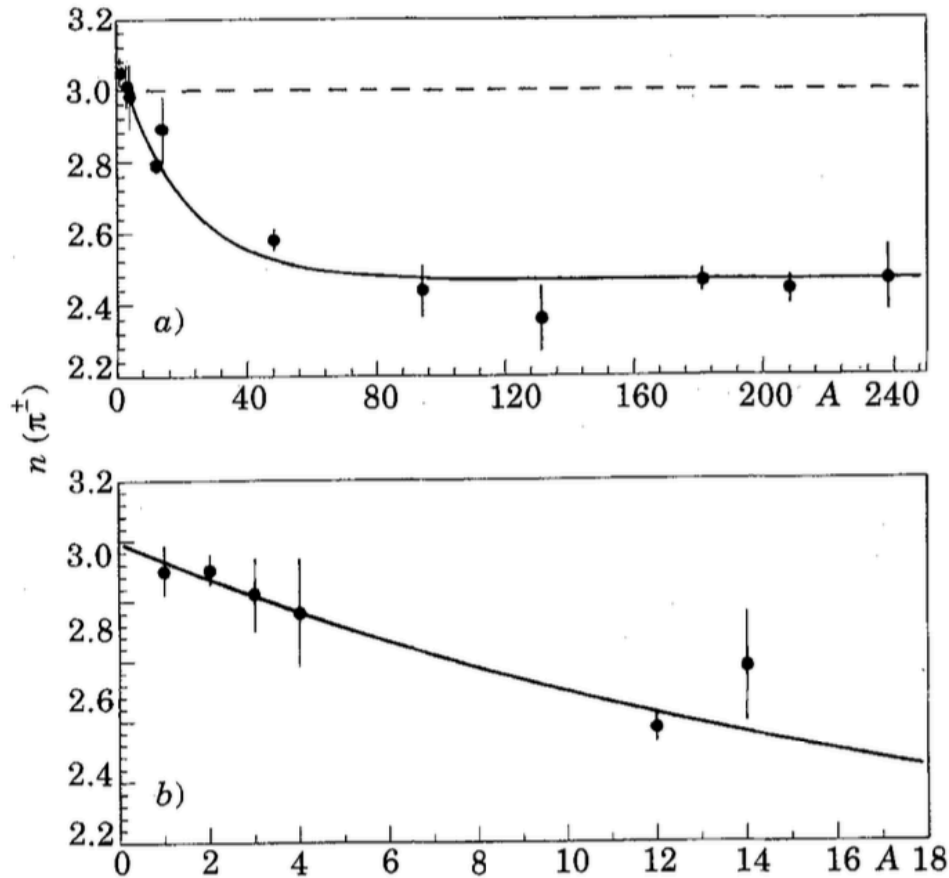
- For annihilation at rest, \bar{p} s are captured in atomic orbits with high principal quantum number and high orbital quantum number ($n \sim 40$) and cascades down emitting Auger electrons and X-rays until it finds itself in an orbit ($n = 9$ to 4, depending on the charge of the nucleus) where it can annihilate with a nucleon.
- The overlap between the \bar{p} wave function and the nucleus will occur mostly at large distances from the centre of the nucleus less than 10% of the central density.
- Because of the high annihilation cross-section \bar{p} s annihilate with high probability on the surface of the nuclei and only a small fraction penetrates deeply into the nuclei.



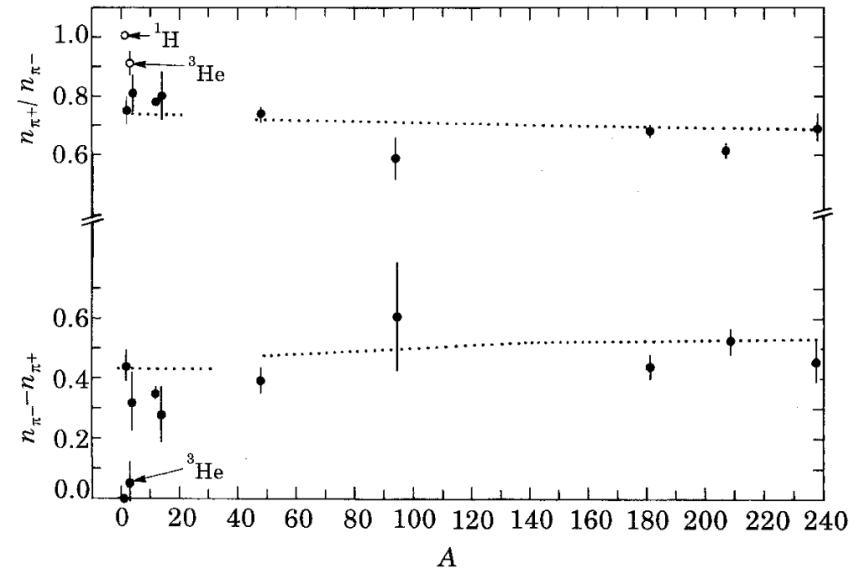
Schematic picture of \bar{p} annihilation on the nuclear surface.

The figure shows the difference between uncorrelated pion production (1) and pion production by heavy mesons (2), where the probability that all pions leave the nucleus is higher.

Pion multiplicity measurements



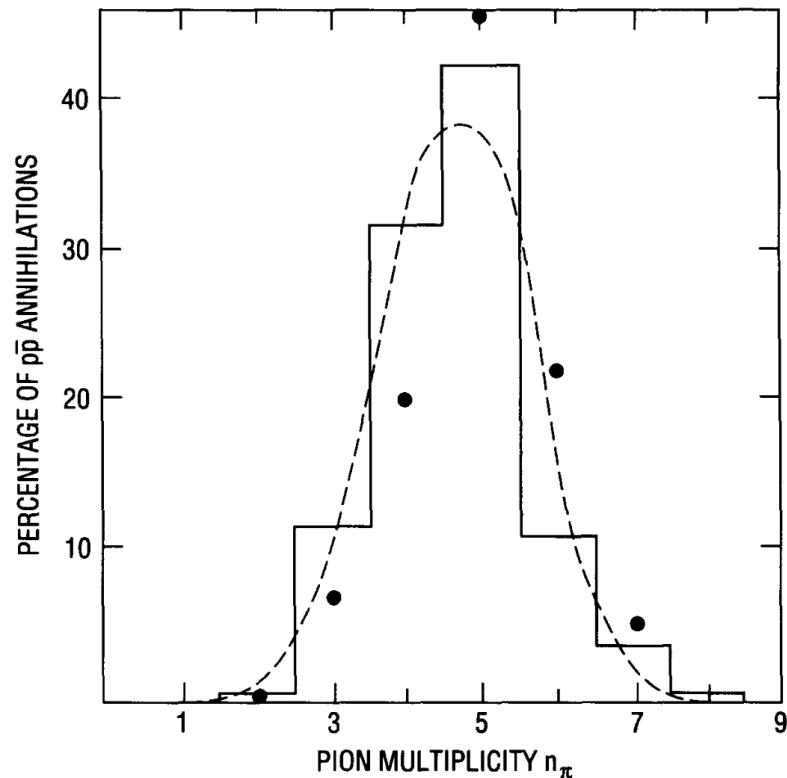
Charged pion multiplicity v/s A . The full line is the result of a best-fit calculation. The dashed line is the behaviour expected neglecting FSI.



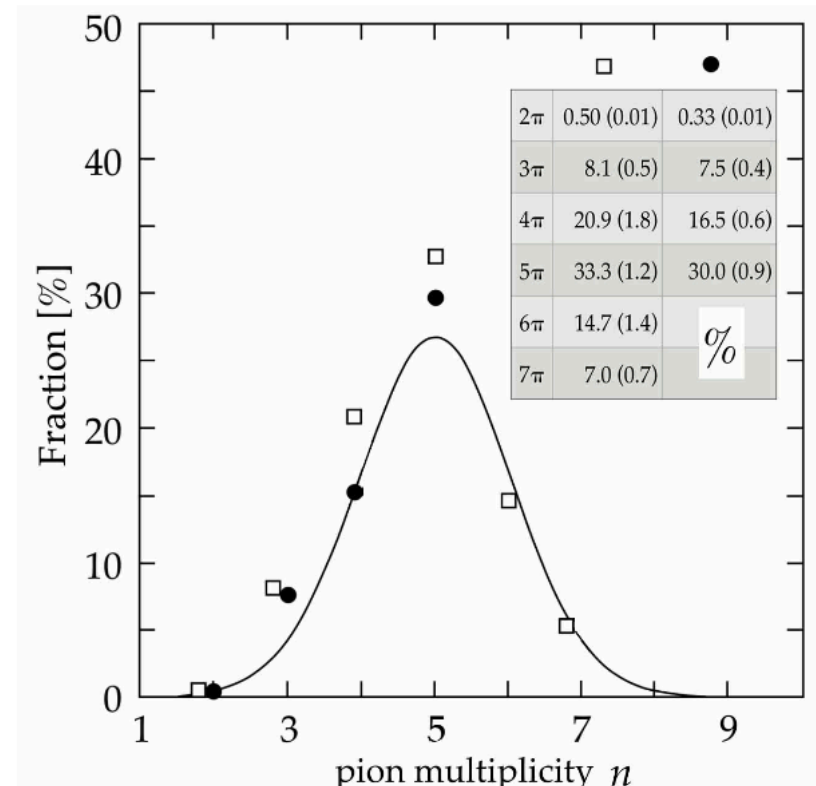
$r = n_{\pi^+}/n_{\pi^-}$ and $d = n_{\pi^+} - n_{\pi^-}$ vs A at rest. The lines give the behaviours when the FSI is neglected.

Bendiscioli, G., Kharzeev, D. Antinucleon-nucleon and antinucleon-nucleus interaction. A review of experimental data. *Riv. Nuovo Cim.* **17**, 1–142 (1994). <https://doi.org/10.1007/BF02724447>

Total pion multiplicity



Pion multiplicity distribution for $p\bar{p}$ annihilation at rest. The histogram represents the prediction of the statistical bootstrap model (Hamer, 1972). The dashed line represents a Gaussian fit with $\langle n \rangle = 4.61$ and $\sigma = 0.95$. The dots correspond to the experimental data. [C. B. DOVER et al., Prog.Part.Nucl.Phys., Vol. 29, pp. 87-173, 1992]



Branching fraction as a function of multiplicity for $p\bar{p}$ annihilation at rest in liquid hydrogen. Full circles: data from bubble chambers and CRYSTAL BARREL. Open squares: expected distribution using the factorial law. The curve is a Gaussian fit assuming the average multiplicity $\langle n \rangle = 5$, $\sigma = 1.04 \pm 0.01$.

Pion multiplicity

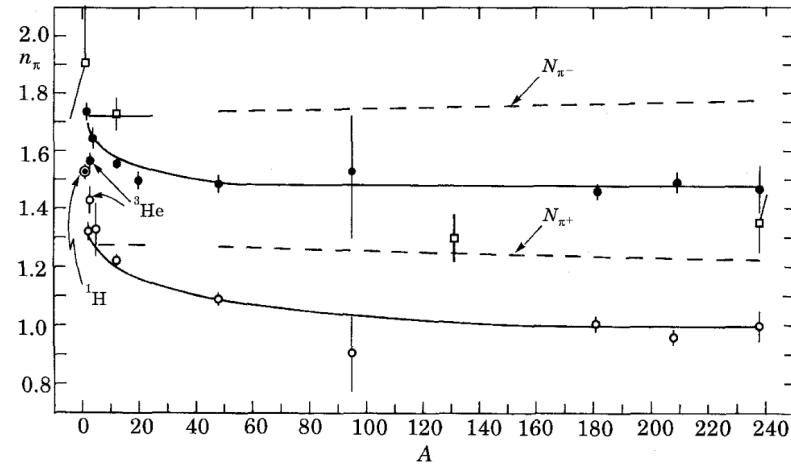
- In \bar{p} annihilation, 5 pions are produced on average, both in correlated and in uncorrelated ways; in the latter way they are produced through heavier mesons (ρ , ω ..) which then decay into pions.
- For $p\bar{p}$ annihilation, an average of 3.0 ± 0.2 charged pions (π^\pm) and 2.0 ± 0.2 neutral pions (π^0) are produced. When the annihilation occurs on a neutron, on average 1.07 ± 0.04 π^+ and 2.07 ± 0.04 π^- are produced.
- The mean pion energy released from \bar{p} annihilation at rest is about 320-350 MeV.
- Pions can undergo charge-exchange reactions with the nucleons or pion absorption reactions which transforms p into n and vice versa and change the relative numbers of π^+ , π^- , π^0 s.
- For annihilations involving more than one nucleon, another possibility is the Pontecorvo reactions, $\bar{p}N \rightarrow M + X + \text{spectator nuclear fragments}$ where M , X are mesons and baryons respectively.



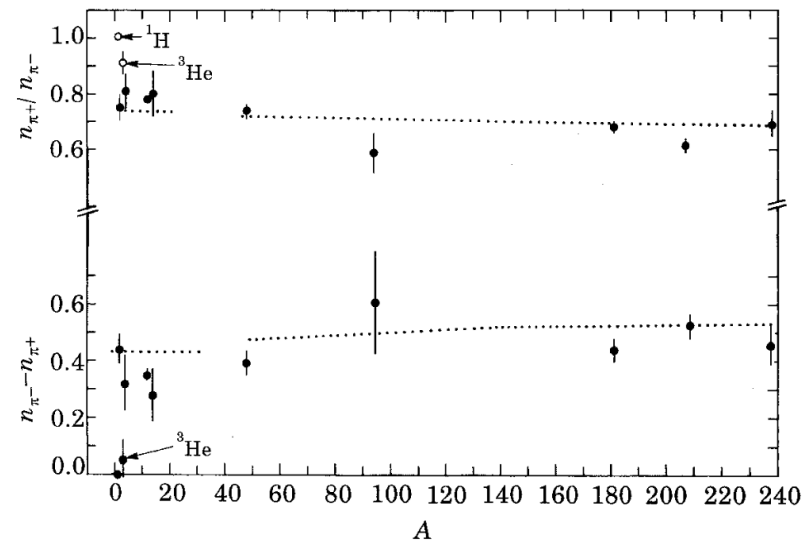
π^+ / π^-

- As a general trend, the production of negative pions is favoured as A increases.
- First, the % of neutrons increases with A and this favours the occurrence of $\bar{p}n$ annihilations which produces on average 1 π^+ and 2 π^- against 1.5 π^+ and 1.5 π^- as in the $p\bar{p}$ annihilations.
- Second, if the number of the neutrons is higher than that of the protons, the charge exchange reactions, $\pi^+n \rightarrow \pi^0p, \pi^0n \rightarrow \pi^-p$ are more favoured than the reverse ones, as well as the absorption reactions, $\pi^+nn \rightarrow pn, \pi^+pn \rightarrow pp$ with respect to $\pi^-pp \rightarrow pn, \pi^-pn \rightarrow nn$.

Therefore, owing to FSI, π^+ should disappear with higher probability than π^- .



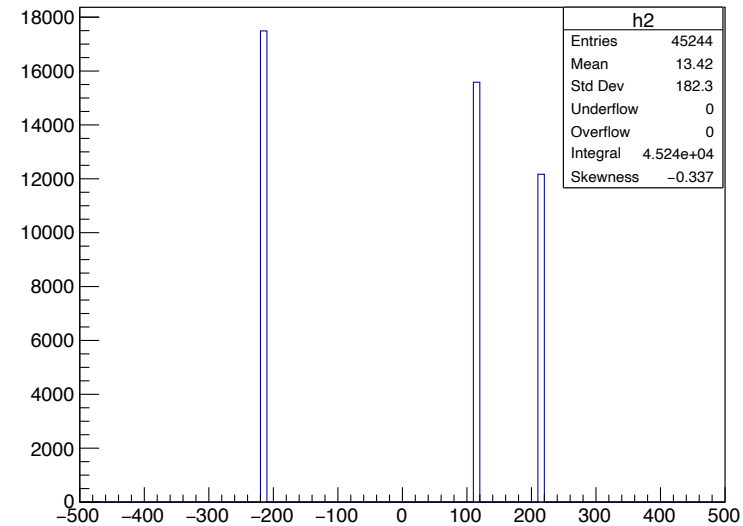
π^- (full circles), π^+ (open circles), π^0 (open squares) mean multiplicity distributions vs. A. The full lines are guides for the eye. The dashed lines give the multiplicities estimated neglecting FSI.



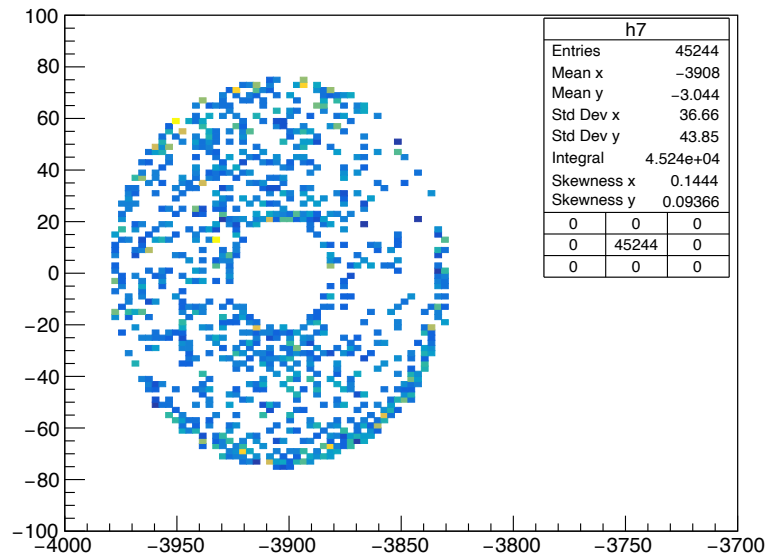
$r = n_{\pi^+}/n_{\pi^-}$ and $d = n_{\pi^-} - n_{\pi^+}$ vs A at rest. The lines give the behaviours when the FSI is neglected.

GEANT4 pions from \bar{p} annihilation

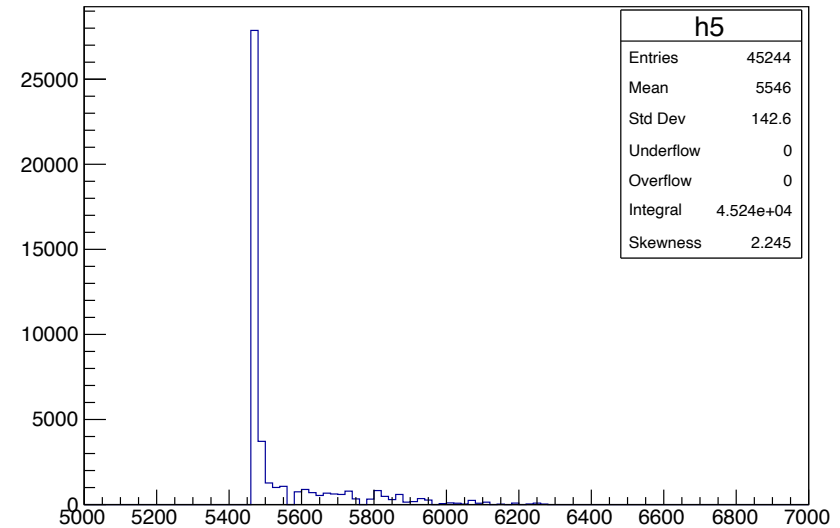
- Most \bar{p} s stop within the first few foils of the ST.
- For 10^4 \bar{p} annihilation at the AI ST events generated, we obtain 17490 π^- , 12170 π^+ and 15584 π^0 with \bar{p} s as their direct mother particle.
- As expected, we obtain about 30% less π^+ than π^- 's.



Pions from 10^4 \bar{p} annihilations at rest.



Starting y v/s x position of the pions (mm).



Starting z position of the pions (mm).

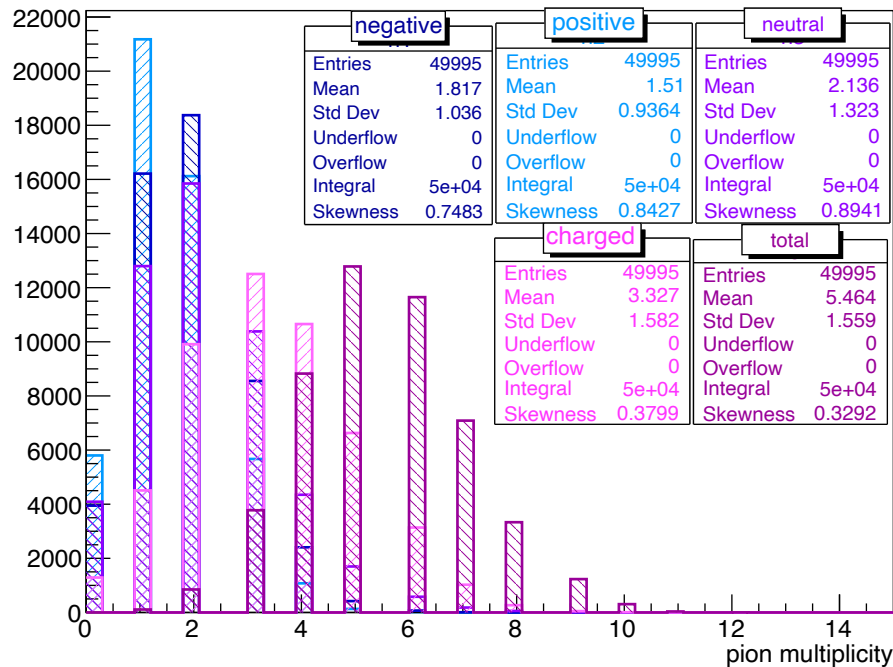
GEANT4 pion multiplicity

1. In 5×10^4 \bar{p} annihilation at rest in the AI ST events, considering all the pions (no selection cuts):

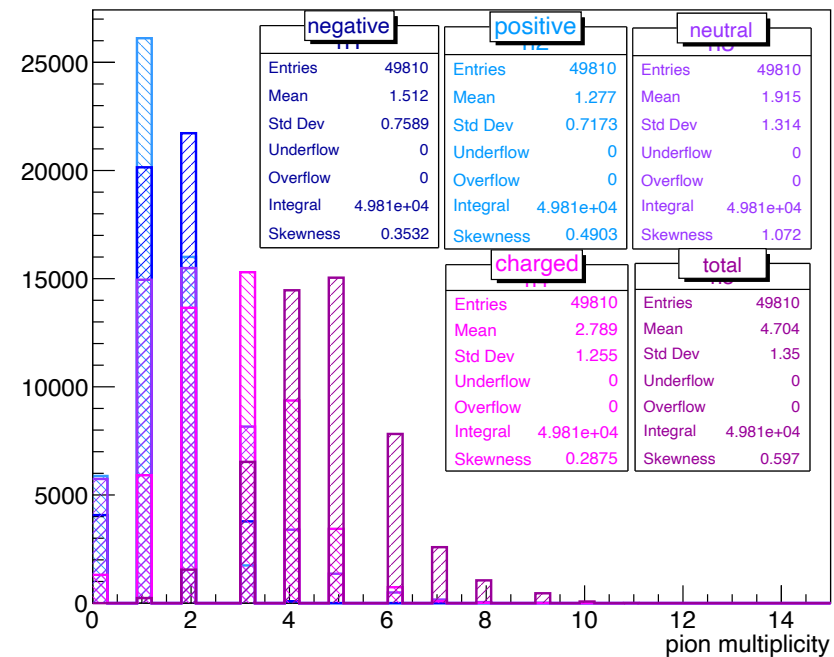
$$\langle n_{\pi^\pm} \rangle = 3.33, \quad \langle n_{\pi^0} \rangle = 2.14, \quad \langle n_\pi \rangle = 5.46.$$

2. If we only consider pions whose starting position is in the ST,

$$\langle n_{\pi^\pm} \rangle = 2.79, \quad \langle n_{\pi^0} \rangle = 1.92, \quad \langle n_\pi \rangle = 4.70.$$



(1)



(2)

Comparison of GEANT4 and experimental data on \bar{p} annihilation

Experiment	X (A, Z)	Charged pions per annihilation	Neutral pions per annihilation	Total number of pions per annihilation	Reference
BC	H (1,1)	3.05 ± 0.04	1.96 ± 0.23	5.01 ± 0.23	[Ghes 74]
BC	H (1,1)	3.06 ± 0.03			[Balt 66]
GTMS	H (2,1)	3.10 ± 0.12			[Ried 89]
SC	He (3,2)	3.01 ± 0.06			[Bend 90]
	He (4,2)	2.97 ± 0.09			[Bale]
SC	He (4,2)	2.98 ± 0.09			[Bale 88b]
MS	C (12,6)	2.84 ± 0.01 (± 0.10)	1.73 ± 0.04 (± 0.10)	4.57 ± 0.04 (± 0.15)	[Arms 89, Mino 90]
	C (12,6)	2.72 ± 0.03			[Wade 76]
GTMS	N (14,7)	2.89 ± 0.09			[Ried 89]
CB	Liq. H2	3.12 ± 0.12	2.07 ± 0.08	5.19 ± 0.15	
BNL, CERN, CB	Liq. H2	3.05 ± 0.04	1.93 ± 0.12	4.98 ± 0.13	[Arms 69, Balt 66, Amsl 03]
STBC	Ti (48,22)	2.58 ± 0.03			[Bugg 73]
PE	Mo (94,42)	2.44 ± 0.07		4.68 ± 0.12	[Eksp 61]
PE	Mo (94,42)			4.9 ± 0.1	[Bale 85]
PE		2.50 ± 0.26			[Chamberlain 58]
GEANT4	Al (27,13)	2.79	1.92	4.70	Pions from ST only
GEANT4*	Al (27, 13)	3.33	2.14	5.46	All

Mean multiplicities of pions emitted from annihilations on different nuclei at rest.

BC = bubble chamber (liquid target); GTMS = gas target in magnetic spectrometer; SC =streamer chamber (gas target); STBC =solid targets in bubble chamber. MS = magnetic spectrometer; PBC = propane bubble chamber; PE = photographic emulsion, CB = Crystal Barrel experiment

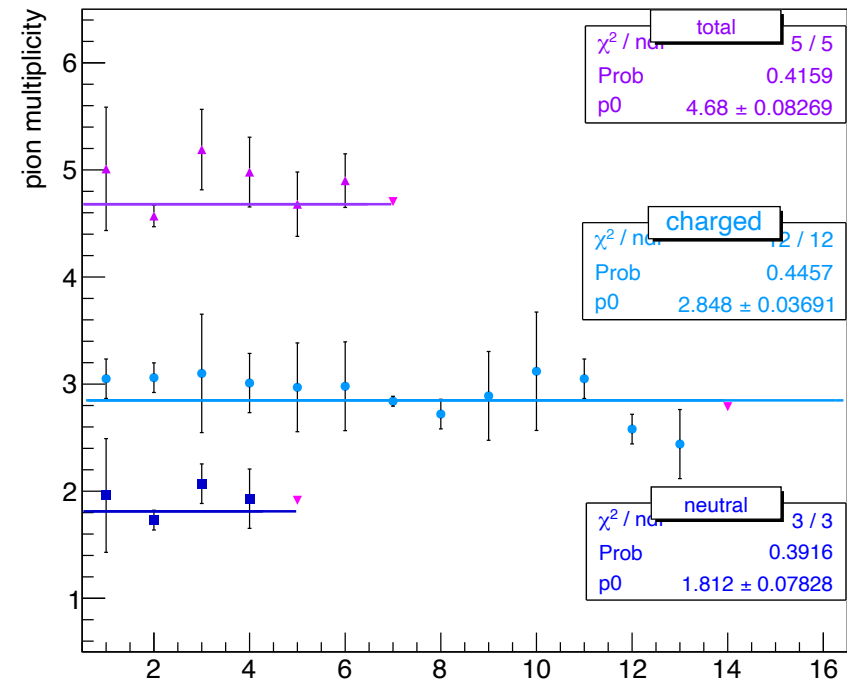
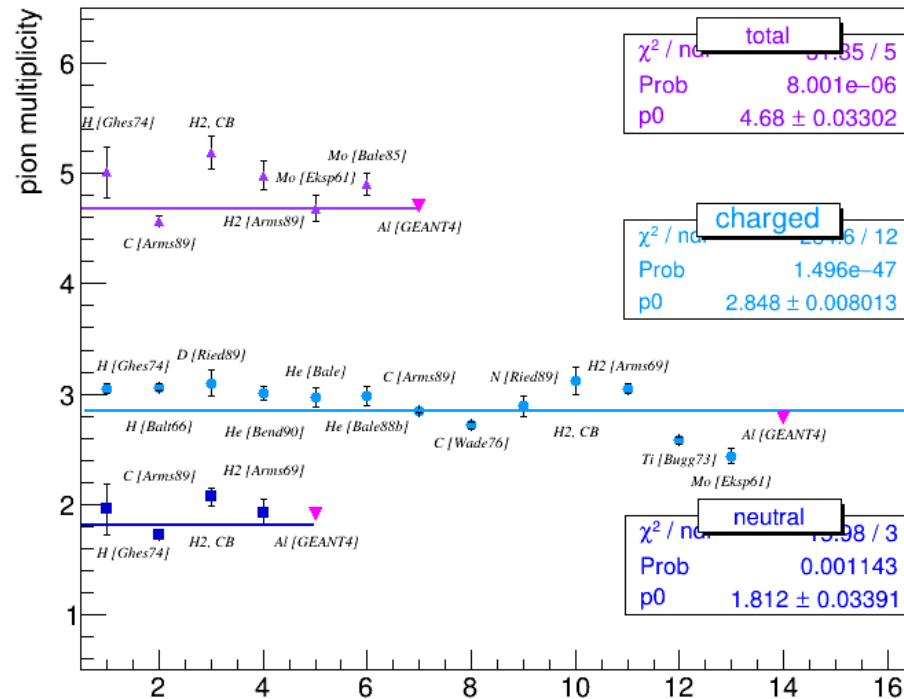
Comparison of GEANT4 and experimental data on \bar{p} annihilation

Experiment, Year	X (A, Z)	Charged pions per annihilation	R	Reference
BC	H (1,1)	3.05 ± 0.04	1.0	[Ghes 74]
BC	H (1,1)	3.06 ± 0.03		[Balt 66]
GTMS	H (2,1)	3.10 ± 0.12	0.75 ± 0.03	[Ried 89]
CB	Liq. H2	3.12 ± 0.12		
BNL, CERN, CB	Liq. H2	3.05 ± 0.04		[Arms 69, Balt 66, Amsl 03]
SC	He (3,2)	3.01 ± 0.06	0.91 ± 0.04	[Bend 90]
	He (4,2)	2.97 ± 0.09	0.81 ± 0.06	[Bale]
SC	He (4,2)	2.98 ± 0.09		[Bale 88b]
MS	C (12,6)	2.84 ± 0.01 (± 0.10)	0.77 ± 0.01	[Arms 89, Mino 90]
	C (12,6)	2.72 ± 0.03		[Wade 76]
GTMS	N (14,7)	2.89 ± 0.09	0.80 ± 0.08	[Ried 89]
STBC	Ti (48,22)	2.58 ± 0.03	0.73 ± 0.02	[Bugg 73]
PE	Mo (94,42)	2.44 ± 0.07	0.59 ± 0.09	[Eksp 61]
GEANT4	Al (27,13)	2.79	0.85	Pions from ST only
GEANT4*	Al (27, 13)	3.33	0.83	

Mean multiplicities of pions emitted from annihilations on different nuclei at rest.

BC = bubble chamber (liquid target); GTMS = gas target in magnetic spectrometer; SC =streamer chamber (gas target); STBC =solid targets in bubble chamber. MS = magnetic spectrometer; PBC = propane bubble chamber; PE = photographic emulsion, CB = Crystal Barrel experiment

Comparison of GEANT4 and experimental data on \bar{p} annihilation

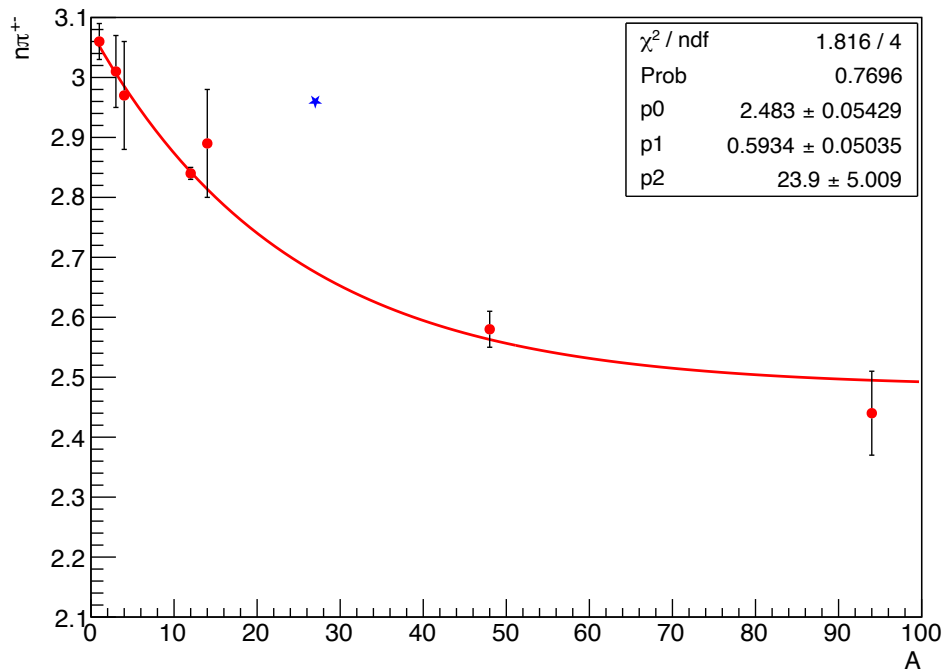


Total, charged and neutral pion multiplicities for various targets/experiments. The GEANT4 multiplicities are given in magenta. **AI [GEANT4], total** refers to the case where all the pions were considered, no selection cuts. **AI [GEANT4]** refers to the case where only pions whose starting position is the ST is considered.

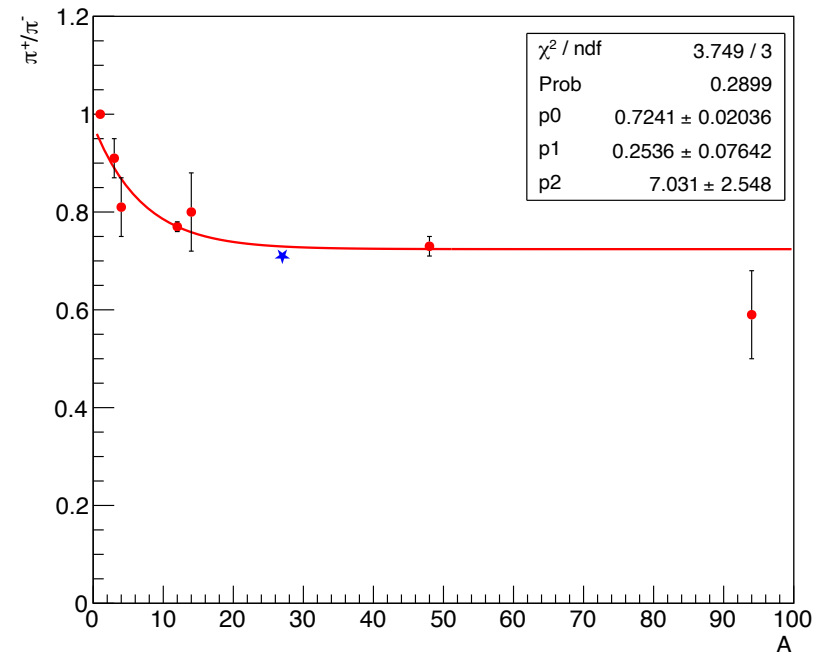
Total, charged and neutral pion multiplicities for various targets/experiments. The GEANT4 multiplicities are given in magenta. The errors are rescaled to force the χ^2/ndf of the straight line fit to 1.0.

- From the fit, the uncertainty on the total pion multiplicity is about 1.7%, on the charged pion multiplicity is 1.4% and 4.4% on the neutral pion multiplicity.

Comparison of GEANT4 and experimental data on \bar{p} annihilation



$n\pi^\pm$ v/s A



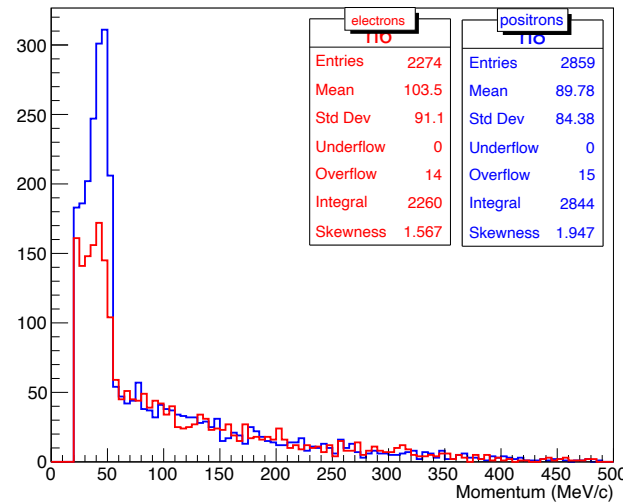
π^+/π^- v/s A

$n\pi^\pm$ v/s A and π^+/π^- v/s A.

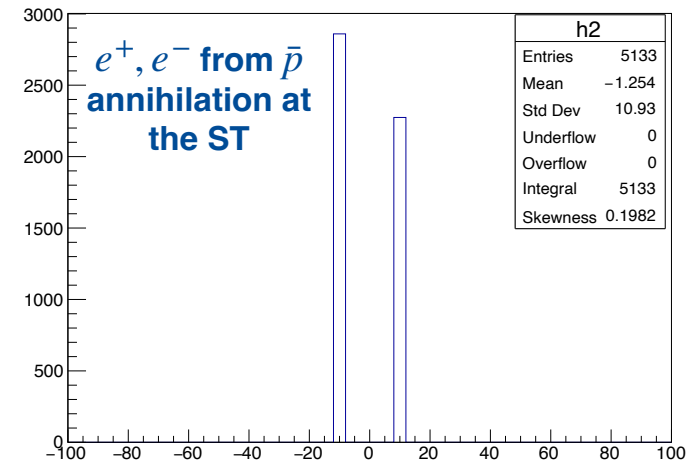
Red: Experimental measurements over the years,
Blue star: GEANT4 value for Al target.

GEANT4 e^- , e^+ momentum distributions

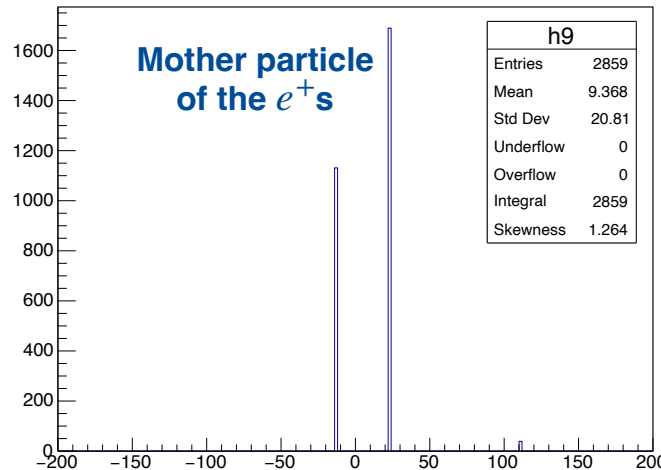
- For $10^4 \bar{p}$ annihilation at the ST events, we obtain a total of 16352 π^+ , 22916 π^- .
- About 57% of π^+ decay into μ^+ , 43% of π^+ undergo inelastic interactions.
- About 22% of π^- decay into μ^- , 31% undergo nuclear capture, 47% π^- perform inelastic interactions.
- Therefore, we have more μ^+ 's than μ^- 's, which leads to about 25% more e^+ than e^- .
- As expected, the e^- 's are produced by $\pi^0 \rightarrow \gamma\gamma$ decays followed by $\gamma \rightarrow e^-e^+$ and $\pi^- \rightarrow \mu^- \bar{\nu}$ decays followed by μ^- decays.



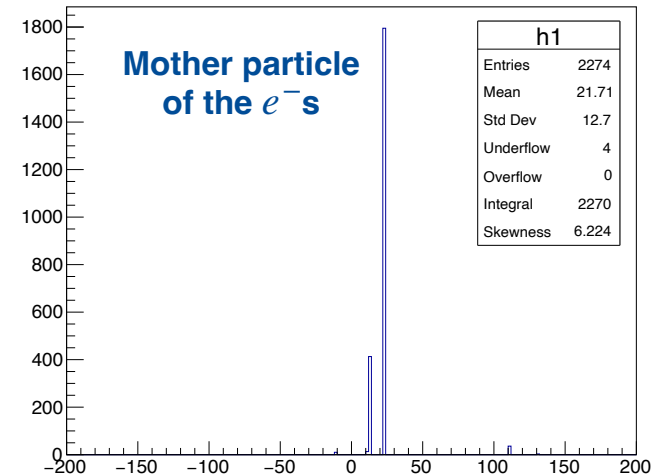
Momentum (MeV/c)



e^+ , e^- from \bar{p} annihilation at the ST



Mother particle of the e^+ 's



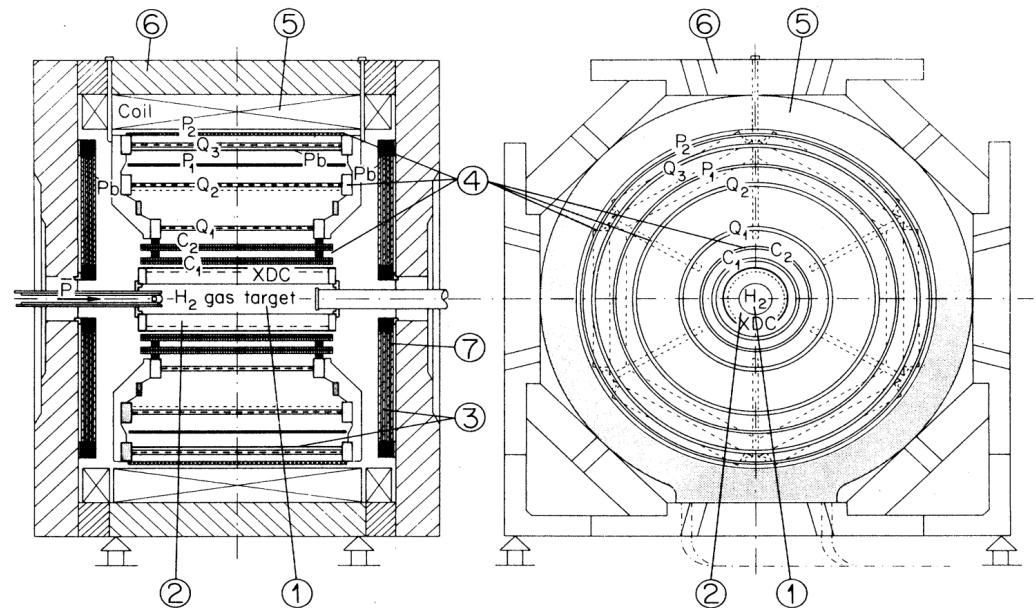
Mother particle of the e^- 's

Systematic Uncertainties II: Pion momentum - shape based estimation

$p\bar{p}$ and $\bar{p}N$ annihilation at rest

J. Riedlberger et al. Antiproton annihilation at rest in nitrogen and deuterium gas. Phys. Rev. C, 40:2717–2731, Dec 1989.

- The ASTERIX experiment was performed at LEAR as well. Gaseous nitrogen and H_2 targets were used.
- The complete data sample comprises 3.3×10^5 and 4.0×10^5 events for nitrogen and hydrogen respectively, taken with the minimum bias \bar{p} stop trigger condition, requiring only the disappearance of a \bar{p} in the target.
- For pions, the acceptance of the spectrometer reached a plateau of 70% for $P > 80$ MeV/c; the minimum detectable momentum was 40 MeV/c. At these low momenta pattern recognition was found to be unreliable, because normally only four track points were seen. Thus the region below 80 MeV/c was excluded.



The ASTERIX spectrometer. (1) Hydrogen (nitrogen) gas target. The small disks at the end and at the entrance are the scintillators defining the incoming \bar{p} and vetoing a nonstopping \bar{p} , respectively. (2) Spiral projection chamber (50% Ar, 50% C_2H_6 gas). (3) Lead foils to convert photons. (4) Cylindrical multiwire proportional chambers; C₁, C₂, Q₁, Q₂, Q₃ with anode (wires parallel to beam axis) and cathode readout (helical strips); P₁, P₂ anode readout only. (5) Coils and (6) yoke to produce a 0.8 Tesla axial field. (7) Endcaps with hexagonal multiwire proportional chambers for position-sensitive photon detection.

$p\bar{p}$ and $\bar{p}N$ annihilation at rest

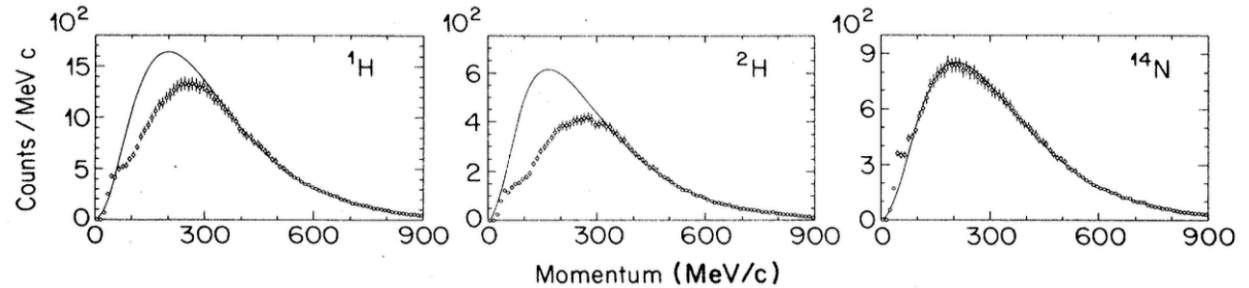
J. Riedlberger et al. Antiproton annihilation at rest in nitrogen and deuterium gas. Phys. Rev. C, 40:2717–2731, Dec 1989.

- For a relativistic Maxwell-Boltzmann distribution the momentum spectrum follows,

$$dN/dp = A(p^2/E) \exp(-E/E_0)$$

where the normalization constant A and the temperature E_0 are experimental parameters.

- For hydrogen and deuterium such a parametrization only describes the pion spectra above $p > 300$ MeV/c, whereas in N_2 the lower limit is 100 MeV/c.



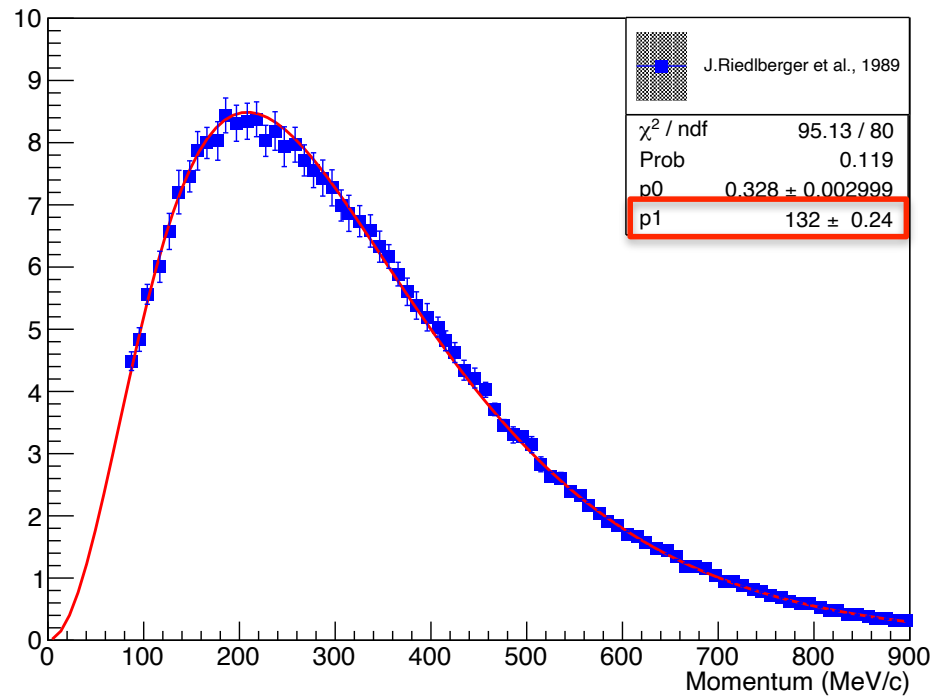
Pion momentum spectra for 1H , 2H and ^{14}N . The curves show the Maxwell-Boltzmann distribution fits to the spectrum.

Target	Channel	Particle	Range of fit (GeV/c)	Parameter	Results	
					This experiment	Other experiments
1H	all	π^\pm	$0.3 \leq p_\pi \leq 0.9$	E_0 (MeV)	128 ± 1	128 ± 1 , Ref. 21
2H		π^-	$0.3 \leq p_\pi \leq 0.9$	E_0 (MeV)	126 ± 1	124 ± 1 , Ref. 21
^{14}N		π^-	$0.1 \leq p_\pi \leq 0.9$	E_0 (MeV)	131 ± 1	
^{12}C		π^-		E_0 (MeV)		136 ± 3 , Ref. 13
2H	all	p	$0.2 \leq p_p \leq 0.9$	E_0 (MeV)	64 ± 1	
^{14}N		p	$0.2 \leq p_p \leq 0.9$	E_0 (MeV)	66 ± 1	
^{12}C		p		E_0 (MeV)		78 ± 4 Ref. 13
2H	$3\pi^- 2\pi^+$	p	$p_p \leq 0.2$	Y_s (%)	79 ± 2	
				μ (MeV/c)	87 ± 2	
			$p_p \geq 0.2$	Y_{MB} (%)	21 ± 2	23 ± 1 , Ref. 54
				E_0 (MeV)	55 ± 1	
2H	$2\pi^- \pi^+$	p	$p_p \leq 0.2$	Y_s (%)	75 ± 2	
				μ (MeV/c)	105 ± 2	
			$p_p \geq 0.2$	Y_{MB} (%)	25 ± 2	25 ± 2 , Ref. 22
				E_0 (MeV)	98 ± 3	80 , Ref. 22

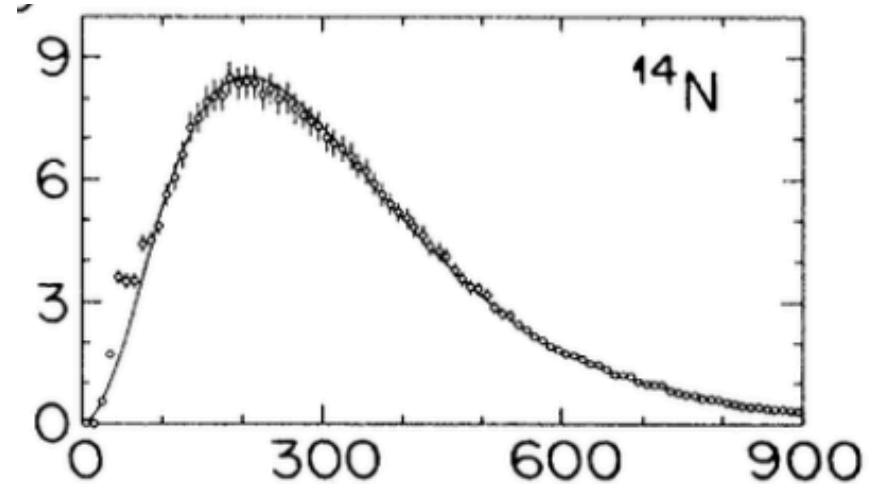
Parameters for the fits of the pion spectra. E_0 : Temperature characteristic for the Maxwell-Boltzmann distribution

Inclusive negative pion momentum spectrum for $\bar{p}N$ annihilation at rest

- As stated in previous slide, “ the minimum detectable momentum was 40 MeV/c in ASTERIX. At these low momenta pattern recognition was found to be unreliable, because normally only four track points were seen. **Thus the region below 80 MeV/c was excluded.** ”



$\chi^2/dof = 1.18$



Target	Channel	Particle	Range of fit (GeV/c)	Parameter	Results	
					This experiment	Other experiments
^1H	all	π^\pm	$0.3 \leq p_\pi \leq 0.9$	E_0 (MeV)	128 ± 1	128 ± 1 , Ref. 21
^2H		π^-	$0.3 \leq p_\pi \leq 0.9$	E_0 (MeV)	126 ± 1	124 ± 1 , Ref. 21
^{14}N		π^-	$0.1 \leq p_\pi \leq 0.9$	E_0 (MeV)	131 ± 1	
^{12}C		π^-		E_0 (MeV)		136 ± 3 , Ref. 13

Event generator: StoppedPbarGun2 module

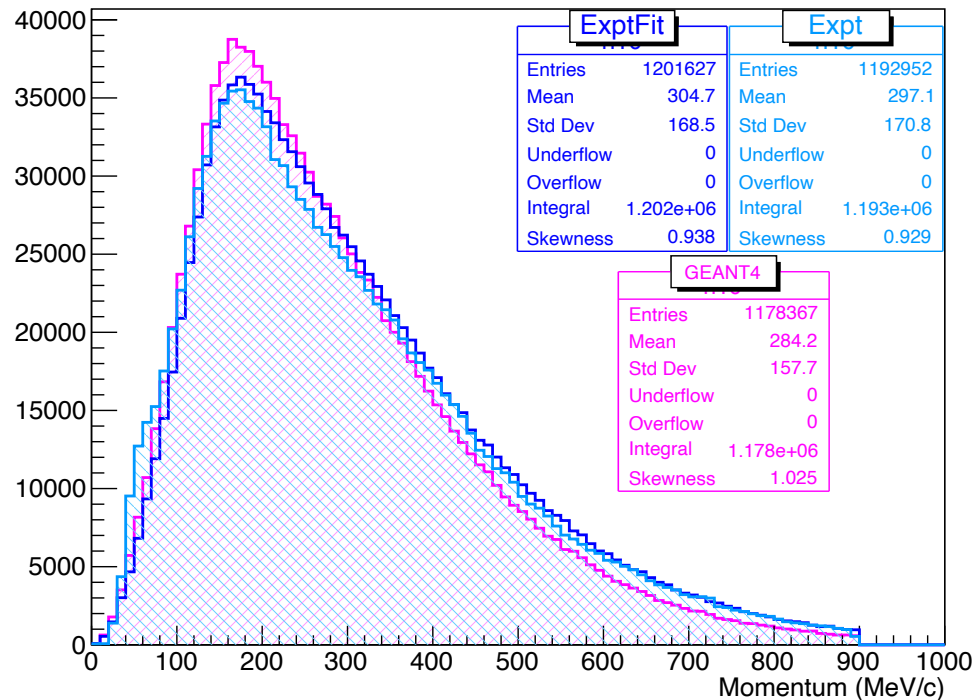
- Objective: Shoot pions following the momentum spectrum given by GEANT4 and experiment and compare the number of signal like electrons obtained in both the cases.
- Initially tried to use some of the EventGenerators present in Offline but could not find an example fcl where an input file was not being used.
- So, made my own version of a particle gun, based on the StoppedParticleReactionGun and StoppedPbarGun (which we use for \bar{p} stops at the ST) modules .
- It is saved as StoppedPbarGun2_module in the pbar2m/src area.
- It is simple. We specify the pdg ID of the particle, the start location of the particles and point to the table of momentum spectrum that the particle must refer to.

```
antiPGun2: {
  module_type      : StoppedPbarGun2
  physics: {
    genId          : pbarFlat
    pdgId          : -211
    spectrumShape  : "tabulated"
    spectrumFileName : "Offline/ConditionsService/data/negativepionmomCarbonexperiment.tbl"
    elow          : 0
    ehi           : 1000
    spectrumVariable: momentum
  }
}
```

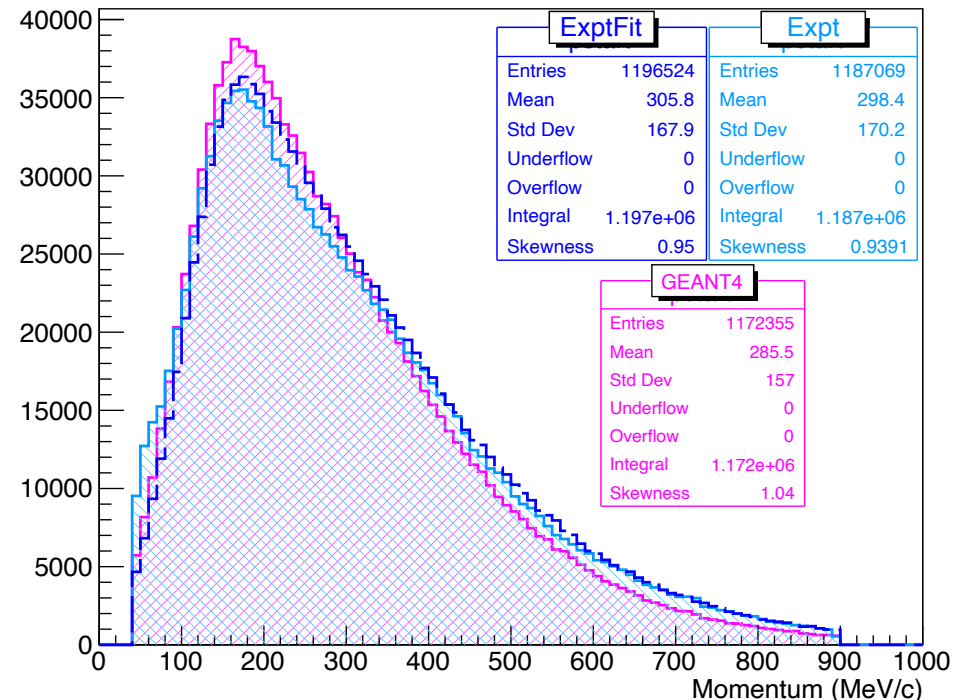
Prolog

$\bar{p}N$ annihilation at rest simulated from the experimental and GEANT4 data as inputs

Magenta: GEANT4, Blue: Experimental data points, Dark blue: Experimental data points fit with Maxwell-Boltzmann spectrum.



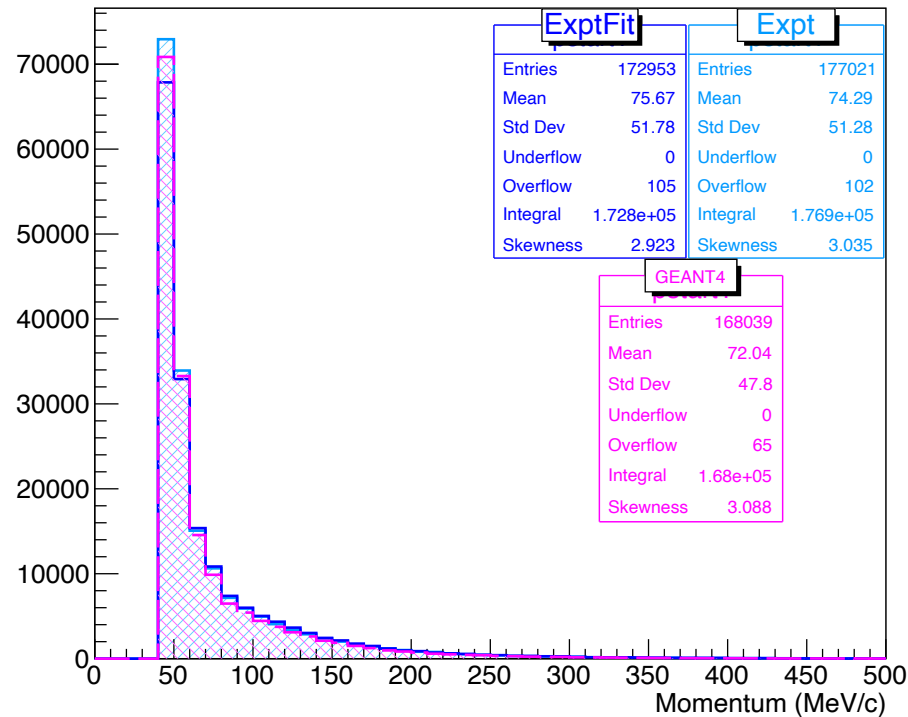
Negative pions (dts)



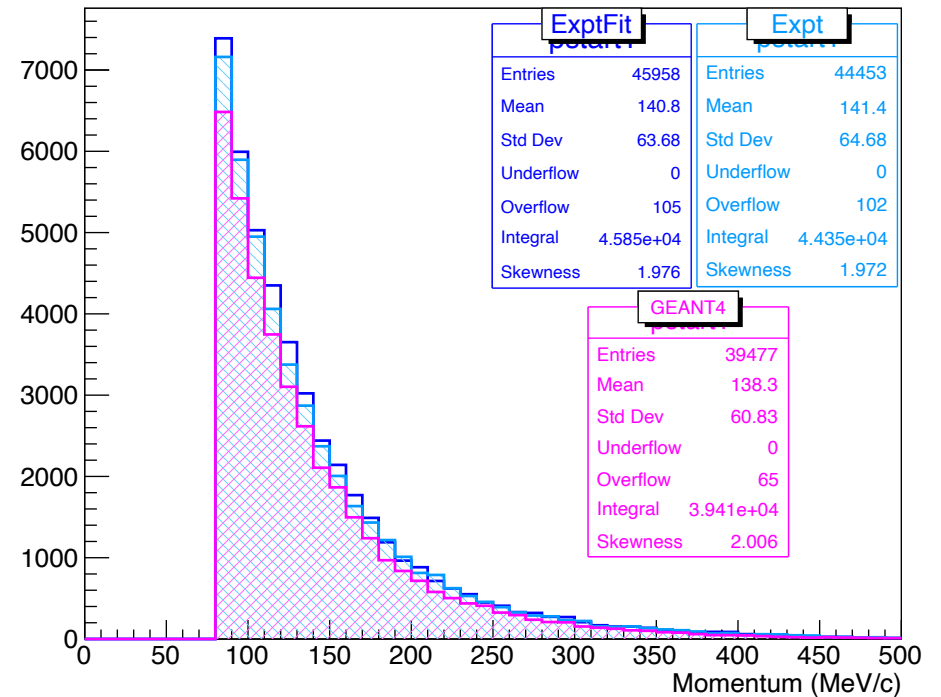
Negative pions (digi)

Electrons from $\bar{p}N$ annihilation at rest simulated from the experimental and GEANT4 data as inputs

Magenta: GEANT4, Blue: Experimental data points, Dark blue: Experimental data points fit with Maxwell-Boltzmann spectrum.



No selection cuts

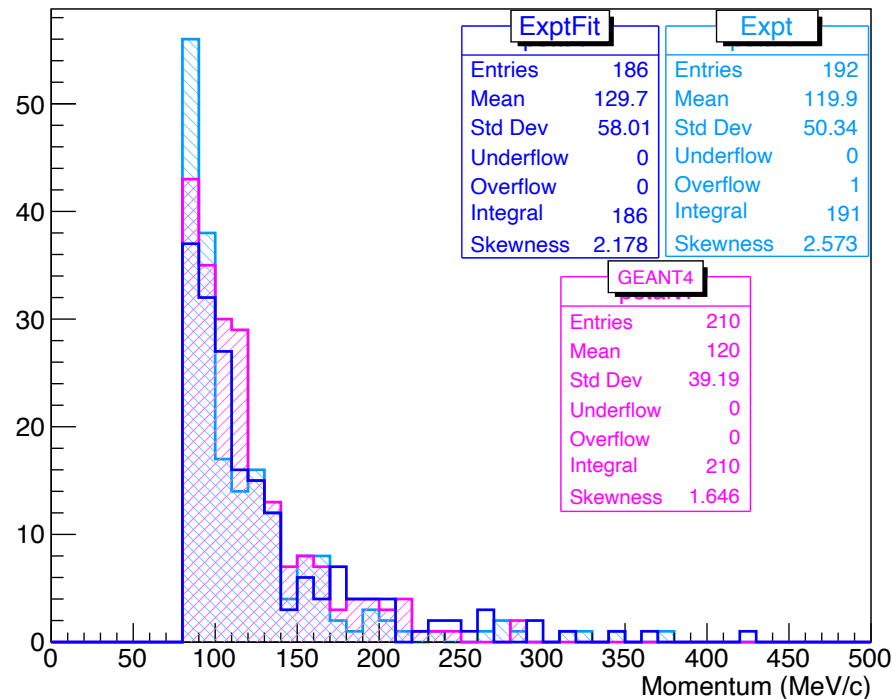


$P \geq 80$ MeV/c

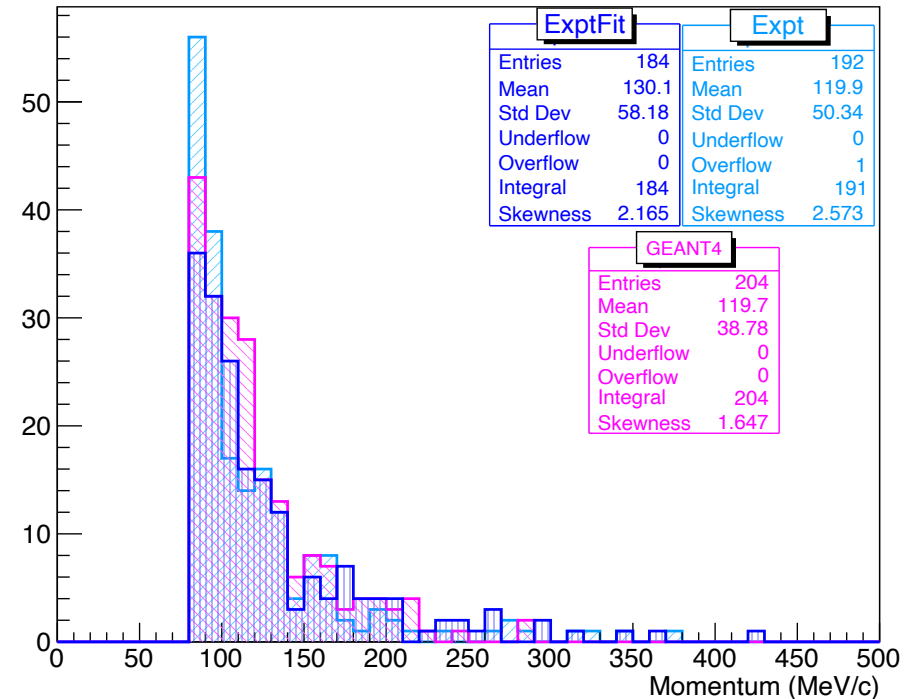
Note: A pion with momentum ~ 60 MeV/c can produce an e^- with $E_{e^-,max} \approx 102.6$ MeV.

Electrons from $\bar{p}N$ annihilation at rest simulated from the experimental and GEANT4 data as inputs

Magenta: GEANT4, Blue: Experimental data points, Dark blue: Experimental data points fit with Maxwell-Boltzmann spectrum.



$P \geq 80, nSH \geq 20$



$P \geq 80, nSH \geq 20, \text{single-electron event}$

Therefore if we consider the region of interest $90 < p < 110$ MeV/c and compare the GEANT4 n_e to the one obtained from the experimental fit n'_e , we obtain an uncertainty of 15%.

Conclusion (Systematic uncertainties)

- From the pion multiplicity comparisons, I have estimated the systematic uncertainty on the charged, neutral and total pion multiplicity as 1.4%, 4.4% and 1.7% respectively for \bar{p} annihilation at rest.
- The pion momentum spectra looked very similar and comparable for simulations and the ones obtained from experiments for various targets.
- Since we are dealing with \bar{p} annihilation at rest in an Al target, the closest comparison I could find was the π^- spectrum obtained for \bar{p} annihilation at rest in a nitrogen target, measured by the ASTERIX experiment.
- After running simulations of 10^6 generated events with the GEANT4 and experimental fit π^- spectra as input respectively, the final number of single-electron events were 204 and 184 events respectively. The shapes of the distributions were comparable as well.
- Therefore if we consider the region of interest $90 < p < 110$ MeV/c and compare the GEANT4 n_e to the one obtained from the experimental fit n'_e , we obtain a systematic uncertainty of 15%.
- Therefore, a total uncertainty of about 15.63%.

PRELIMINARY

\bar{p} background study documentation

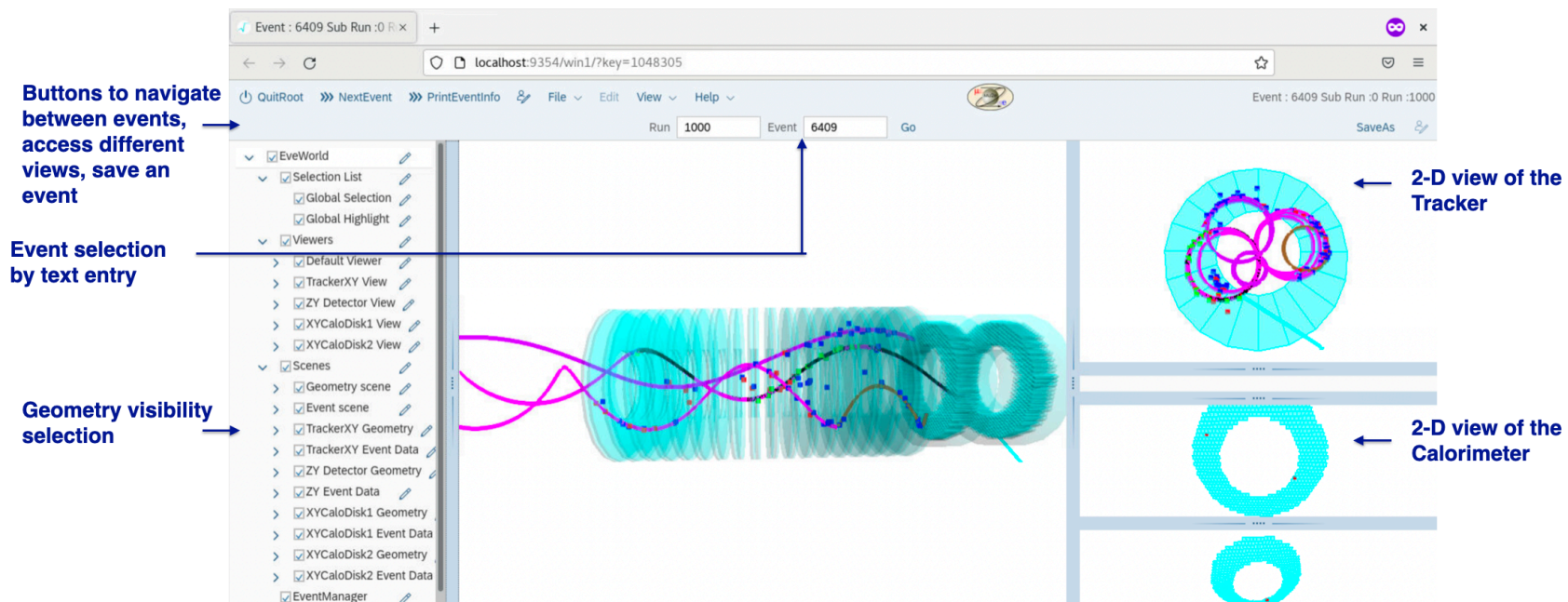
- Multi-track event reconstruction to constrain the \bar{p} background in Mu2e Nuclear Instruments and Methods in Physics Research Section A: Accelerators, Spectrometers, Detectors and Associated Equipment Vol. 1069, December 2024
<https://doi.org/10.1016/j.nima.2024.169937>
- A data-driven method to constrain the \bar{p} background in Mu2e Il Nuovo Cimento C, Vol. 47, Issue 5, Article 281, 5 August 2024
<https://doi.org/10.1393/ncc/i2024-24281-x>
- Developing a data-driven method to constrain the antiproton background in the Mu2e experiment Il Nuovo Cimento C, Vol. 47, Issue 3; Conference: Incontri di Fisica delle Alte Energie - IFAE 2023, Catania, Sicily (Italy), 12-14 Apr 2023, 03 April, 2024
<https://doi.org/10.1393/ncc/i2024-24110-4>
- Mu2e DocDB: 51152, 50889, 49668, 49647, 48066, 46365 etc.
- <https://github.com/Mu2e/pbar2m/blob/main/doc/pbar2m.org>

Service Tasks:

**Event display development, Offline and
pbar2m repository maintenance,
Tracker electronics installation and
DAQ**

Event display for Mu2e

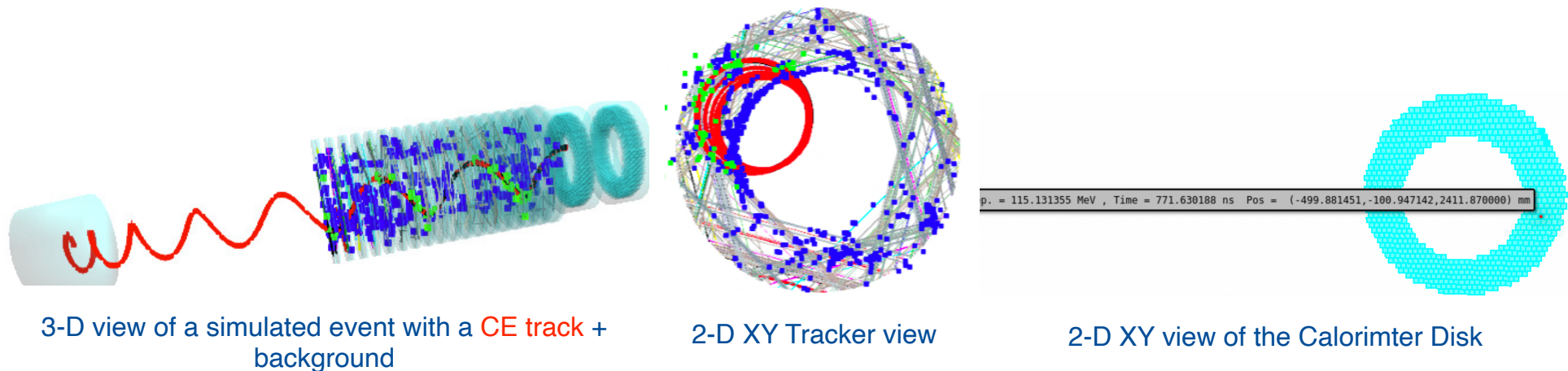
- Event display is the top layer of a robust framework. It helps to visualise the physics in each event.
- Crucial for monitoring and debugging during live data taking, offline analysis as well as public outreach.
- A custom, offline display prototype was first developed using **TEve**, a ROOT based 3-D event visualisation framework.
- The online display is being developed using **Eve-7**, an upgraded version of TEve which allows remote access for live data taking.
- Multiple Users can simultaneously view and interact with display.



Main window of the online event display
Given here is an example event of $p\bar{p}$ annihilation at the ST in the DS

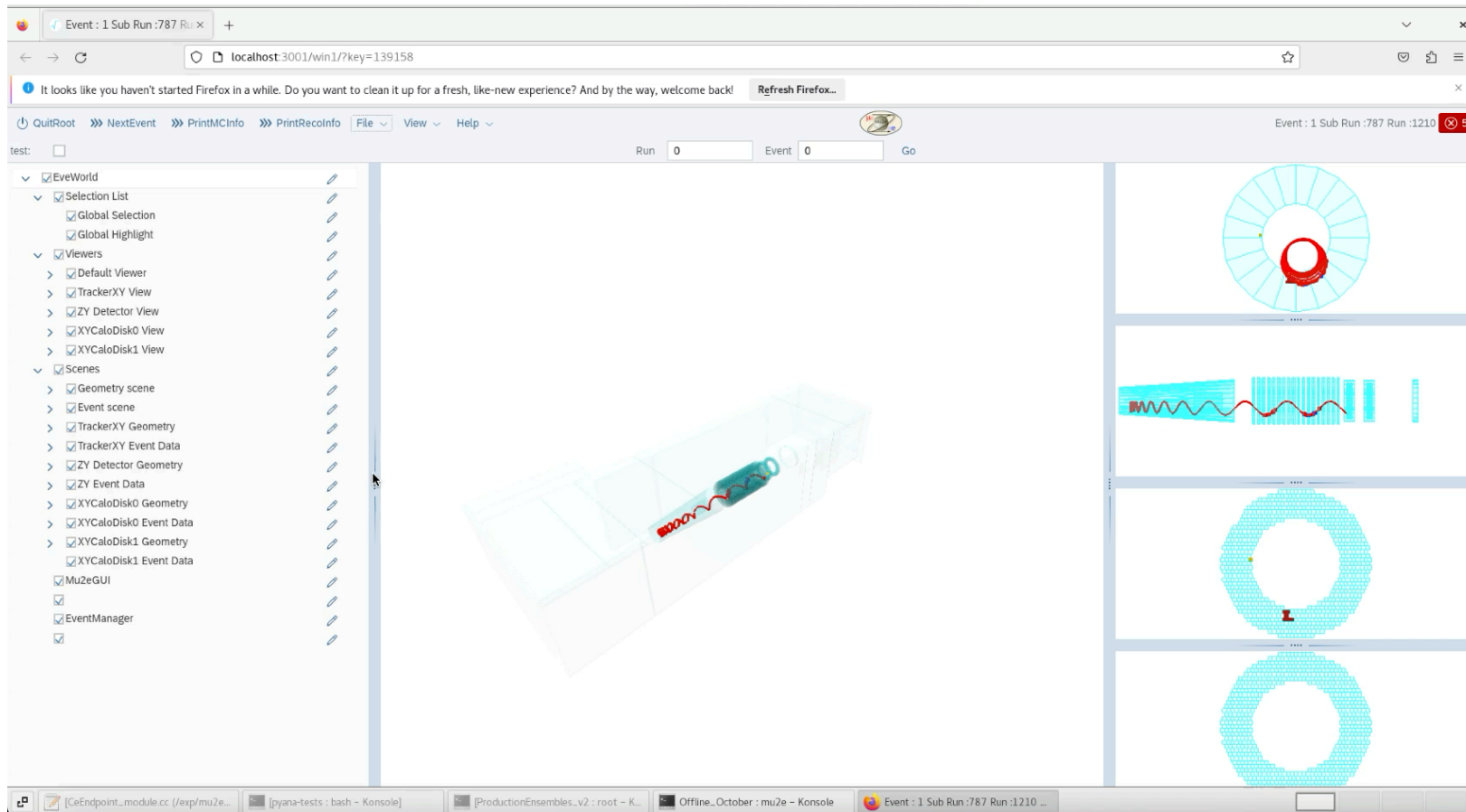
Features of the online display

- Reconstructed data like the tracks, hits and clusters can be displayed within the detector geometries upon GUI request.
- User defined track selection and colour coding feature, utilising the particle ID. For example : **e-**, **e+**, μ^- , π .
- The “hits” used in the track reconstruction are highlighted in **green** while the unused hits are in **blue**.
- Relevant information about the simulated particle, reconstructed track, straw and calorimeter crystal “hits” can be obtained on tool-tip.

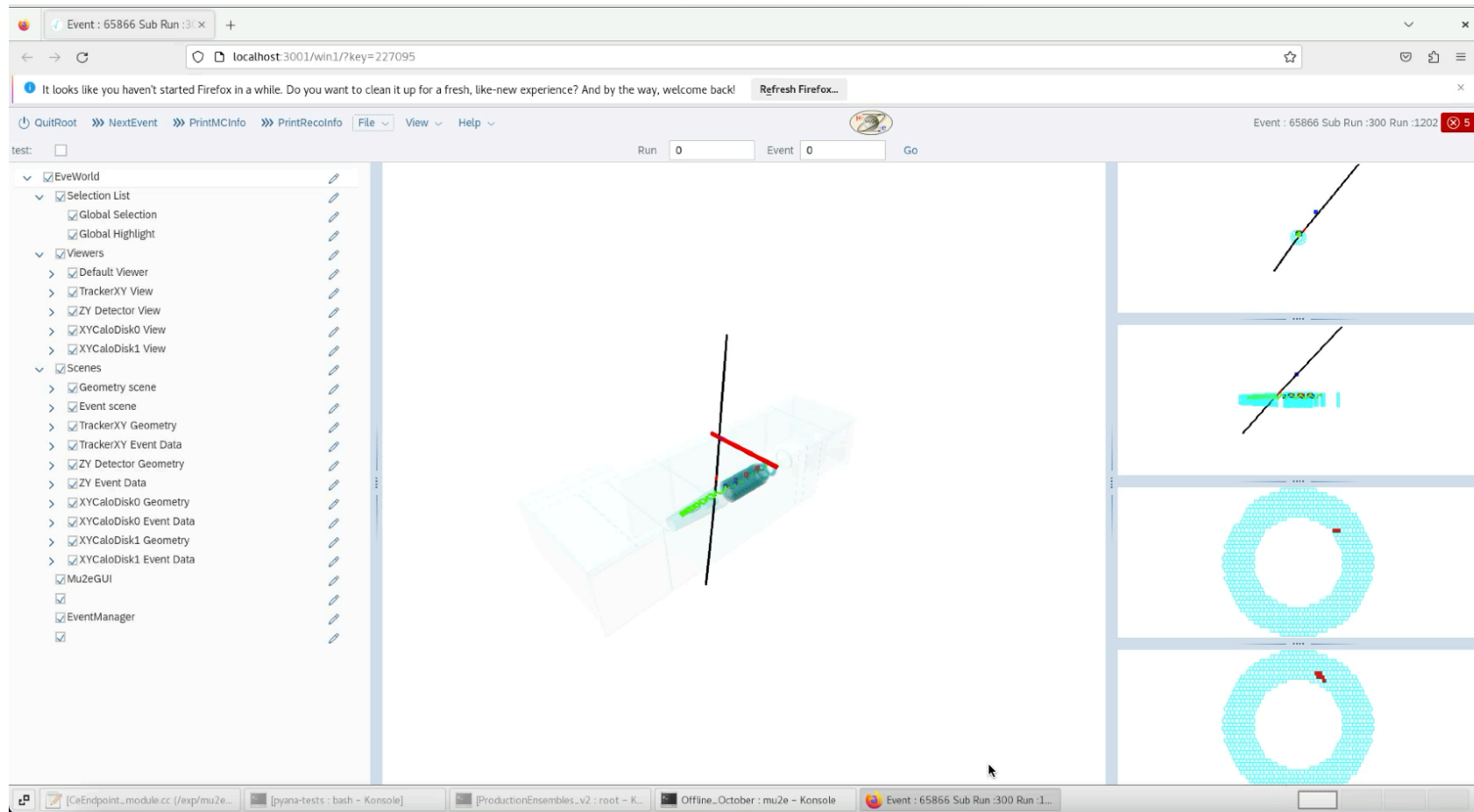


- The MC truth and reconstructed tracks can be displayed together, allowing visualisation of the track resolution.
- A GUI “ShowCRV” option is added which lets the user view the CRV geometry and the cosmic muon tracks and hits.

Event display for Mu2e



Event display for Mu2e



Event display Documentation

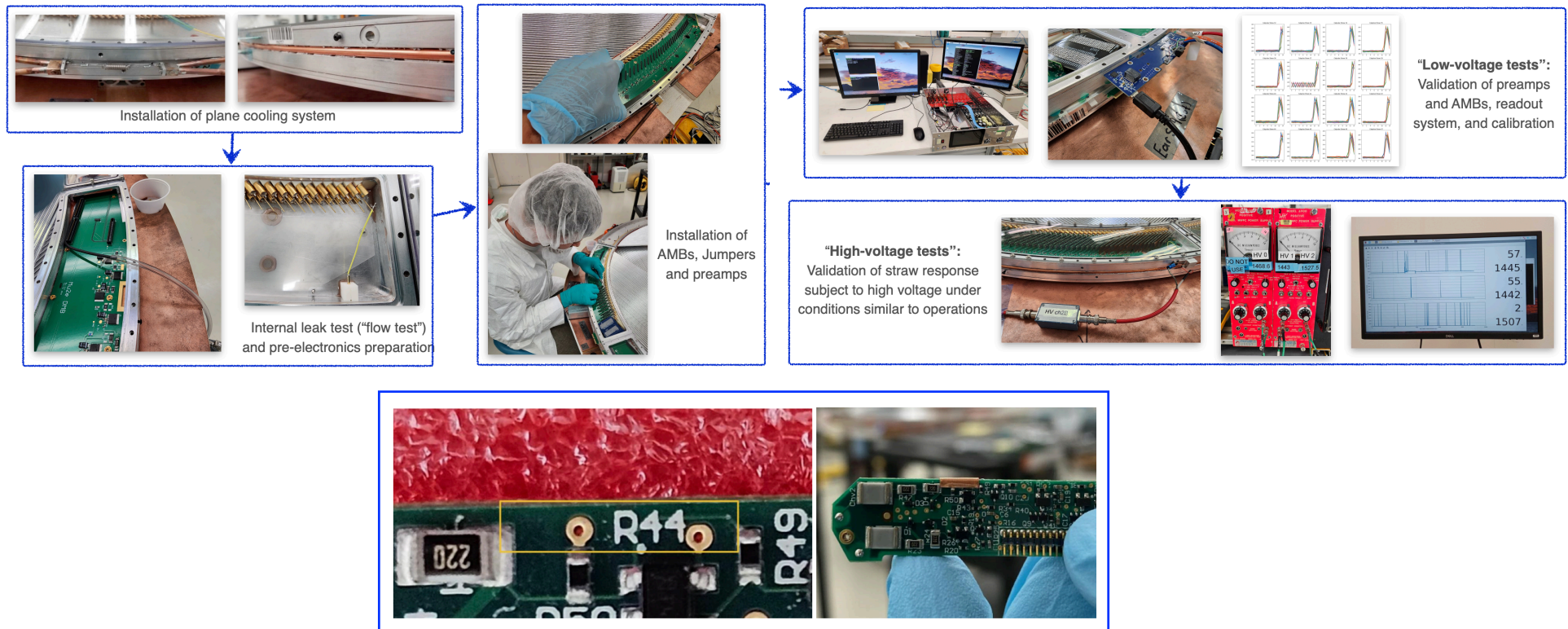
- Mu2e event visualisation development using TEve and Eve-7 Nuclear Instruments and Methods in Physics Research Section A: Accelerators, Spectrometers, Detectors and Associated Equipment, Vol. 1045, 1 January 2023
<https://doi.org/10.1016/j.nima.2022.167614>
- Bulletin of the American Physical Society, X09. 007, April 2022
<https://ui.adsabs.harvard.edu/abs/2022APS..APRX09007C/abstract>
- 21st International Workshop on Advanced Computing and Analysis Techniques in Physics Research 2022, Bari, (Accepted, IOPScience)
<https://indico.cern.ch/event/1106990/papers/4998027/>
- Mu2e DocDB: 50608, 50050, 49166, 48675, 42334, 41538 etc.
- https://mu2ewiki.fnal.gov/wiki/Eve7EventDisplay#Examples_of_the_Eve-7_Mu2e_Display

Offline repository maintenance (Code Management)

- The Mu2e Offline goes through rapid changes and it often results in breaks and incompatibilities with your private analysis repositories and codes.
- I have been maintaining a safe branch of the Offline repository <https://github.com/NamithaChitrazee/Offline/tree/pbar2m> for the 'pbar2m' group (Mu2e Pisa and Yale group students) with the help of Pasha, since Aug 2022.
- We update it every couple of weeks/months as necessary, solve the incompatibilities, validate the results using CE and \bar{p} datasets and release it for the rest of the group.
- We maintain a record of the validation at /mu2e/data/projects/pbar2m/validation/ and update on DocDB as well.
- Further, we maintain the <https://github.com/Mu2e/pbar2m/tree/main> repository (in SU2020 style) where all the code and dataset generation information and fcl files are kept.

Tracker electronics installation and DAQ

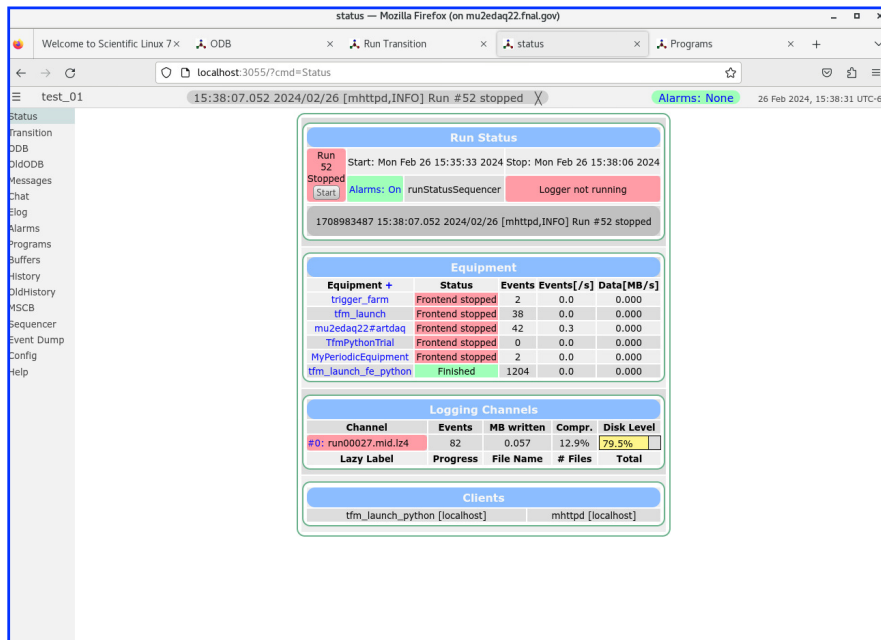
- Assisted in the installation and testing of the production electronics: Pre-amplifiers, Analog motherboards, Jumper boards and DRACs in some of the tracker panels.
- Tested the quality of the installed electronics parts with Low and High voltage testing.
- Helped in the preamp cleaning and addition of copper clips to the preamps to reduce the noise caused by an oscillating electronic feedback due to the lack of shielding on one of the transistors.



Refer to Mu2e DocDB 47702, 46529, 46532 for detailed descriptions

General DAQ development efforts

- Developed the script for starting/stopping a run using the browser (MIDAS based) and launching the farm manager and frontend
https://github.com/pavel1murat/frontends/blob/main/tfm_frontend/tfm_launch_fe.py
- Developed the script for taking the run number from the database during the launch of a new run and updating the database accordingly.



The screenshot shows a web interface for monitoring a run. The main content area is divided into several sections:

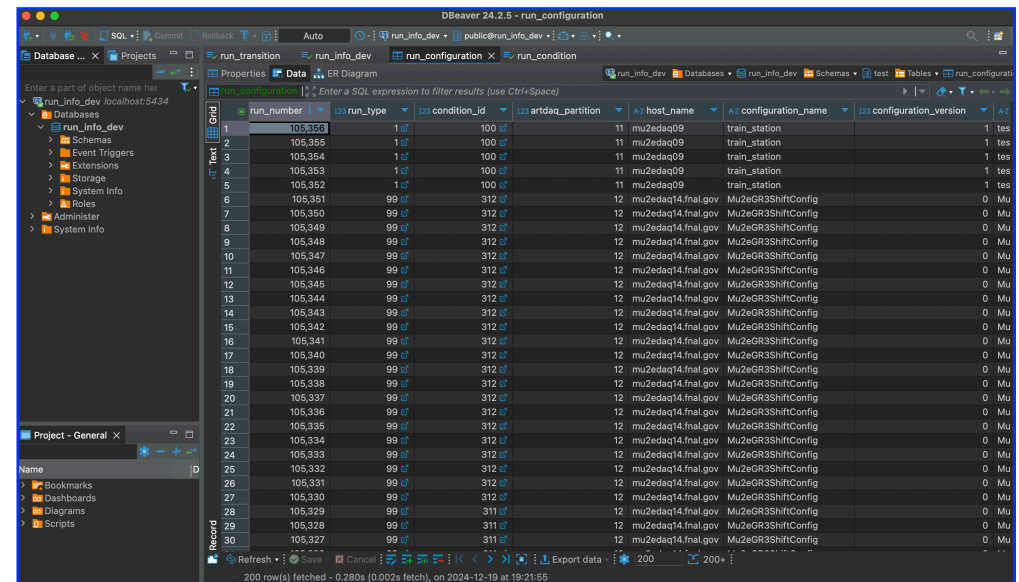
- Run Status:** Shows 'Run 52 Stopped' with a start time of 'Mon Feb 26 15:35:33 2024' and a stop time of 'Mon Feb 26 15:38:06 2024'. It also indicates 'Alarms: On' and 'runStatusSequencer' is running, while 'Logger' is not running.
- Equipment:** A table listing various equipment components and their status.
- Logging Channels:** A table showing logging activity for a specific channel.
- Clients:** A table listing active clients.

Equipment +	Status	Events	Events[/s]	Data[MB/s]
trigger_farm	Frontend stopped	2	0.0	0.000
tfm_launch	Frontend stopped	38	0.0	0.000
mu2edaq22#artdaq	Frontend stopped	42	0.3	0.000
TfmPythonTrial	Frontend stopped	0	0.0	0.000
MyPeriodicEquipment	Frontend stopped	2	0.0	0.000
tfm_launch_fe_python	Finished	1204	0.0	0.000

Channel	Events	MB written	Compr.	Disk Level
#0: run00027.mid.gz4	82	0.057	12.9%	79.5%

Client	Progress	File Name	# Files	Total
tfm_launch_python [localhost]		mhttpd [localhost]		

Page to start/stop the run



The screenshot shows a database viewer displaying a table with the following columns: run_number, run_type, condition_id, artdaq_partition, host_name, configuration_name, and configuration_version. The table contains 30 rows of data, showing various run configurations across different hosts and conditions.

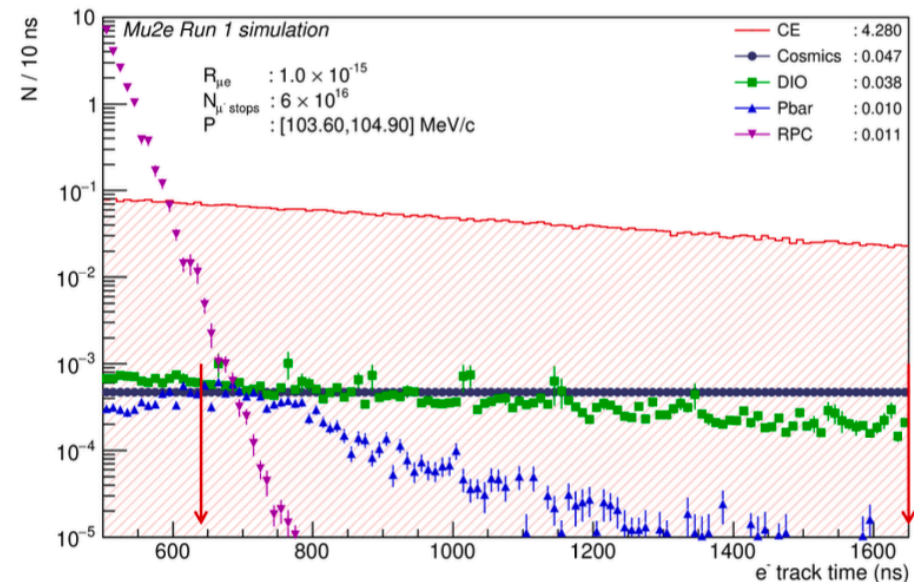
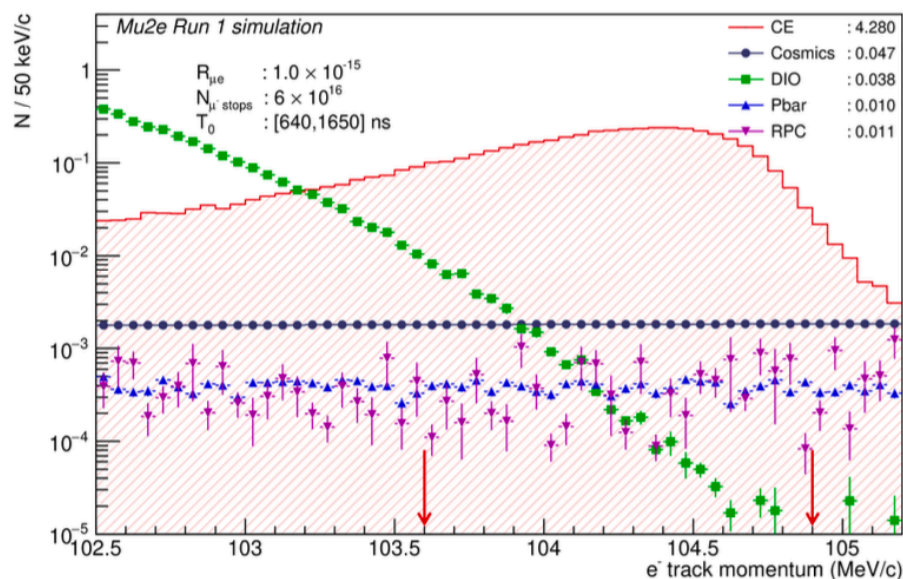
run_number	run_type	condition_id	artdaq_partition	host_name	configuration_name	configuration_version
1	105356	100	100	mu2edaq09	train_station	1 tes
2	105355	100	100	mu2edaq09	train_station	1 tes
3	105354	100	100	mu2edaq09	train_station	1 tes
4	105353	100	100	mu2edaq09	train_station	1 tes
5	105352	100	100	mu2edaq09	train_station	1 tes
6	105351	99	312	mu2edaq14.fnal.gov	Mu2eGRShiftConfig	0 Mu
7	105350	99	312	mu2edaq14.fnal.gov	Mu2eGRShiftConfig	0 Mu
8	105349	99	312	mu2edaq14.fnal.gov	Mu2eGRShiftConfig	0 Mu
9	105348	99	312	mu2edaq14.fnal.gov	Mu2eGRShiftConfig	0 Mu
10	105347	99	312	mu2edaq14.fnal.gov	Mu2eGRShiftConfig	0 Mu
11	105346	99	312	mu2edaq14.fnal.gov	Mu2eGRShiftConfig	0 Mu
12	105345	99	312	mu2edaq14.fnal.gov	Mu2eGRShiftConfig	0 Mu
13	105344	99	312	mu2edaq14.fnal.gov	Mu2eGRShiftConfig	0 Mu
14	105343	99	312	mu2edaq14.fnal.gov	Mu2eGRShiftConfig	0 Mu
15	105342	99	312	mu2edaq14.fnal.gov	Mu2eGRShiftConfig	0 Mu
16	105341	99	312	mu2edaq14.fnal.gov	Mu2eGRShiftConfig	0 Mu
17	105340	99	312	mu2edaq14.fnal.gov	Mu2eGRShiftConfig	0 Mu
18	105339	99	312	mu2edaq14.fnal.gov	Mu2eGRShiftConfig	0 Mu
19	105338	99	312	mu2edaq14.fnal.gov	Mu2eGRShiftConfig	0 Mu
20	105337	99	312	mu2edaq14.fnal.gov	Mu2eGRShiftConfig	0 Mu
21	105336	99	312	mu2edaq14.fnal.gov	Mu2eGRShiftConfig	0 Mu
22	105335	99	312	mu2edaq14.fnal.gov	Mu2eGRShiftConfig	0 Mu
23	105334	99	312	mu2edaq14.fnal.gov	Mu2eGRShiftConfig	0 Mu
24	105333	99	312	mu2edaq14.fnal.gov	Mu2eGRShiftConfig	0 Mu
25	105332	99	312	mu2edaq14.fnal.gov	Mu2eGRShiftConfig	0 Mu
26	105331	99	312	mu2edaq14.fnal.gov	Mu2eGRShiftConfig	0 Mu
27	105330	99	312	mu2edaq14.fnal.gov	Mu2eGRShiftConfig	0 Mu
28	105329	99	311	mu2edaq14.fnal.gov	Mu2eGRShiftConfig	0 Mu
29	105328	99	311	mu2edaq14.fnal.gov	Mu2eGRShiftConfig	0 Mu
30	105327	99	311	mu2edaq14.fnal.gov	Mu2eGRShiftConfig	0 Mu

Run Database

Back-up Slides

Expected sensitivity

- Mu2e Run I assumes an integrated flux of 6×10^{16} muons.
- The optimised signal window if $t_0 \in [640, 1650]$ ns and $p \in [10.6, 104.9]$ MeV/c.
- Single-Event-Sensitivity of 2.3×10^{-16} and a total signal selection efficiency of 11.7%.
- The expected Run I 5σ discovery sensitivity is $R_{\mu e} = 1.2 \times 10^{-15}$.
- If no signal, the expected upper limit is $R_{\mu e} < 6.2 \times 10^{-16}$ at 90% CL.



Minimum muon momentum to obtain a 105 MeV/c electron

- Muon decay at rest $\mu^- \rightarrow e^- \bar{\nu}_e \nu_\mu \Rightarrow E_{e^-,max} = 52.8 \text{ MeV}/c$.
- Total energy of μ with momentum p_μ , $E_\mu = \sqrt{(p_\mu c)^2 + (m_\mu c^2)^2}$.
- If the e^- takes away the maximum energy in the decay process, then $E_{e^-,max} = \gamma(E_{e,max} + \beta p_{e,max} c)$ where $\gamma = E_\mu / m_\mu c^2$.
- For pion decay at rest, $\pi^- \rightarrow \mu^- \nu_\mu$, $p_{\mu,rest} = \frac{m_\pi^2 - m_\mu^2}{2m_\pi} \approx 29.8 \text{ MeV}/c$
- For a pion with momentum p_π , $E_\pi = \sqrt{(p_\pi c)^2 + (m_\pi c^2)^2}$, $\gamma = E_\pi / m_\pi c^2$.
- The muon momentum p_μ can be obtained as $p_\mu = \gamma(p_{\mu,rest} + \beta E_{\mu,rest} / c)$

Minimum muon momentum to obtain a 105 MeV/c electron

- Therefore, say we have a pion with momentum 60 MeV/c,
 $E_\pi = 151.95 \text{ MeV}$, $\gamma = 1.088$, $\beta = 0.39$, $p_\mu \approx 76.9 \text{ MeV}/c$, $E_\mu \approx 130$ MeV.
- Then the resultant e^- energy is $E_{e^-,max} \approx 102.6$ MeV where $\gamma = 1.23$, $\beta = 0.58$.

- If we have a pion with momentum 63 MeV/c, $E_\pi = 153.16$ MeV, $\gamma = 1.097$,
 $\beta = 0.41$, $p_\mu \approx 81.7$ MeV/c, $E_\mu \approx 132.97$ MeV.
- Then the resultant e^- energy is $E_{e^-,max} \approx 107.3$ MeV where $\gamma = 1.27$,
 $\beta = 0.61$.

Final estimation

- From the MC studies for the SU2020 paper,
 $N_{\bar{p}}^{STOPPED} = 180 \pm 15(stat) \pm 180(syst)$ for Run 1.
- The \bar{p} background estimated for Run 1 using the optimised signal momentum and time window of $103.60 < p < 104.90$ MeV/c and $640 < T_0 < 1650$ ns is $0.010 \pm 0.002(stat) \pm 0.001(syst)$.
- From GEANT4 simulations, we have estimated $\frac{N_{e-perMeV}}{N_{multi-trks}} = \frac{1}{500}$ where $N_{e-perMeV}$ is the number of single electrons per MeV in $90 < p < 110$ MeV/c momentum range and $N_{multi-trks}$ is the number of events with > 1 particle track with $p > 80$ MeV/c.

Final estimation

- We reconstruct 217/500 multi-track events, giving a reconstruction efficiency of about 43%.
- We expect the contribution of the \bar{p} background in Mu2e to be very very small. In an ideal situation, we hope to observe 0 multi-track events.
- Therefore, assuming the background follows poisson distribution, if we reconstruct 0 multi-track events in Run 1:

$$P(N_{reco} = 0 | N_{data}) = e^{-\epsilon \times N_{data}}$$

where $\epsilon = 43\%$

- At 90% C.L,

$$P(N_{reco} = 0 | N_{data}) = e^{-\epsilon \times N_{data}} = 0.1$$
$$N_{data} = 5.30$$

- $N_{e-perMeV} = \frac{N_{data}}{500} = \frac{5.3}{500} = 0.0106$ (the upper limit)

Final estimation

N (multi-trk reco)	Lambda	N (multi-trk data)	N (e- per MeV)
0	2.3026	5.3548	0.0107
1	3.8897	9.0458	0.0181
2	5.3223	12.3774	0.0226
3	6.6808	15.5367	0.0311
4	7.9936	18.5897	0.0371
5	9.2747	21.5690	0.0431

At 90%CL, assuming poisson distribution, the upper limits

$$P(x = k) = \frac{\lambda^k e^{-\lambda}}{k!}, \text{ CDF} = e^{-\lambda} \sum_{j=0}^k \frac{\lambda^j}{j!}$$

$\lambda = \epsilon \times N_{multi-trkdata}$ where ϵ is the reconstruction efficiency